

1 **TITLE**

2 Immune checkpoint proteins are conserved across 160 million years of evolution and are
3 expressed on transmissible cancers

4 **RUNNING TITLE**

5 Transmissible cancers express evolutionarily conserved immune checkpoint molecules

6 **AUTHORS**

7 Andrew S. Flies^{1*}, Jocelyn M. Darby¹, Patrick R. Lennard^{1,2}, Peter R. Murphy^{1,3}, Chrissie E. B.
8 Ong¹, Terry L. Pinfold⁴, A. Bruce Lyons⁴, Gregory M. Woods¹, Amanda L. Patchett¹

9 **AFFILIATIONS**

10 ¹Menzies Institute for Medical Research, College of Health and Medicine, University of
11 Tasmania, Hobart, TAS 7000, Australia

12 ²The Roslin Institute and Royal School of Veterinary Studies, University of Edinburgh, Easter
13 Bush Campus, Midlothian, EH25 9RG, UK

14 ³University of Queensland Diamantina Institute, The University of Queensland, Translational
15 Research Institute, Woolloongabba, Queensland, Australia

16 ⁴School of Medicine, College of Health and Medicine, University of Tasmania, Hobart, TAS
17 7000, Australia

18 **CORRESPONDING AUTHOR CONTACT INFORMATION**

19 **Andrew S. Flies, PhD**

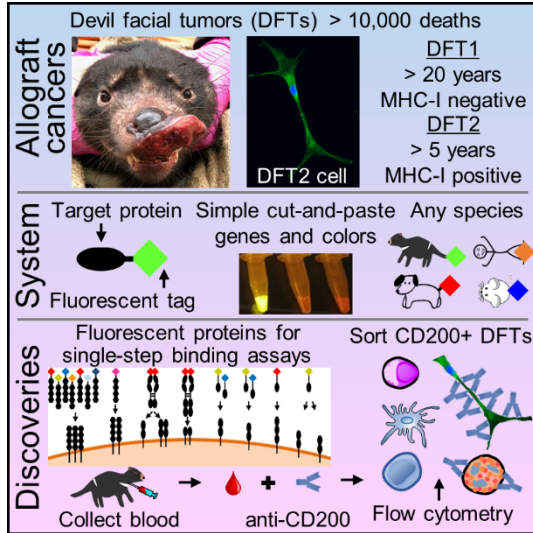
20 Menzies Institute for Medical Research, College of Health and Medicine

21 University of Tasmania

22 Private Bag 23, Hobart TAS 7000

23 phone: +61 3 6226 4614; email: Andy.Flies@utas.edu.au

24 **GRAPHICAL ABSTRACT**



25

26

27 **SIGNIFICANCE**

28 Immune checkpoint immunotherapy has revolutionized medicine, but translational success for
29 new treatments remains low. Around 40% of humans and Tasmanian devils (*Sarcophilus*
30 *harrisii*) develop cancer in their lifetime, compared to less than 10% for most species.
31 Additionally, devils are affected by two of the three known transmissible cancers in mammals.
32 Unfortunately, little is known about the role of immune checkpoints in devils and other non-
33 model species, largely due to a lack of species-specific reagents. We developed a simple cut-and-
34 paste reagent development method applicable to any vertebrate species and show that immune
35 checkpoint interactions are conserved across 160 million years of evolution. The inhibitory
36 checkpoint molecule CD200 is highly expressed on devil facial tumor cells. We are the first to
37 demonstrate that co-expression of CD200R1 can block CD200 expression. The evolutionarily
38 conserved pathways suggest that naturally occurring cancers in devils and other species can
39 serve as models for understanding cancer and immunological tolerance.

40

41 **ABSTRACT**

42 Around 40% of humans and captive Tasmanian devils (*Sarcophilus harrisii*) develop cancer,
43 compared to less than 10% for most species. Tasmanian devils also suffer from two of the three
44 known naturally-occurring transmissible cancers detected in vertebrate species. Transmissible
45 cancers are a unique form of cancer in which tumor cells act as an infectious pathogen and an
46 allograft. The two different transmissible devil facial tumors (DFT1 and DFT2) overcome
47 immunological barriers (e.g. major histocompatibility complex) and have killed thousands of
48 devils. Immune checkpoint immunotherapy has revolutionized human oncology in recent years.
49 However, immune checkpoints in transmissible and non-transmissible cancers remains largely
50 unexplored in most species due to a lack of species-specific reagents. To overcome this, we
51 developed a "cut-and-paste" Fluorescent Adaptable Simple Theranostic (FAST) protein system,
52 adaptable for any vertebrate species. This method facilitated rapid confirmation of seven
53 receptor-ligand interactions between twelve immune checkpoint proteins in Tasmanian devils,
54 thus filling a 160 million year gap in our understanding of the evolution of the mammalian
55 immune system. We used this system to investigate the checkpoint molecule CD200, which can
56 inhibit natural killer cell responses to cancer and facilitate graft tolerance in humans and mice.
57 CD200 was highly expressed on DFT cells and can be used to identify DFT cells in devil blood.
58 Understanding how transmissible tumor cells graft onto new hosts and evade immune defenses
59 will help to identify evolutionarily conserved immunological principles relevant to transplant
60 immunology, cancer, and infectious disease for human and veterinary medicine.

61 **KEYWORDS**

62 immune checkpoint, wild immunology, reagent development, marsupial, transmissible cancer

63 INTRODUCTION

64 Metastatic cancer affects most mammals, but the cancer incidence can vary widely across
65 phylogenetic groups and species (**Figure 1, Table S1**)¹⁻⁹. In humans, the lifetime risk of
66 developing cancer is around 40%¹⁰. This is in stark contrast to a general cancer incidence of 3%
67 for mammals, 2% for birds, and 2% for reptiles reported by the San Diego Zoo (n=10,317)^{7,11}. A
68 more recent study at the Taipei Zoo reported cancer incidence of 8%, 4%, and 1% for mammals,
69 birds, and reptiles, respectively (n=2,657)⁴. Cancer incidence in domestic animals is generally
70 less than 10% (n=202,277)⁹. However, two studies performed 40 years apart reported that
71 greater than 40% of Tasmanian devils develop spontaneous, often severe neoplasia in their
72 lifetime^{11,12}. Devils are also unique because they are affected by two of the three known
73 naturally-occurring transmissible cancers in vertebrate species^{13,14}. Transmissible cancers are a
74 distinct form of cancer in which the tumor cells function as an infectious pathogen and an
75 allograft. Dogs (*Canis lupus familiaris*) are the only other vertebrate species affected by a
76 transmissible cancer¹⁵, and interestingly some breeds of dogs also have high cancer incidence
77^{9,16}.

78 The devil facial tumor (DFT) disease was first detected in Northwest Tasmania and has
79 been a primary driver of an 80% decline in the wild Tasmanian devil population^{13,17}. The clonal
80 devil facial tumor (DFT1) cells have been continually transmitted among devils and is estimated
81 to have killed at least 10,000 individuals since at least 1996. In 2014 a second independent
82 transmissible Tasmanian devil facial tumor (DFT2) was discovered in wild devils¹⁴ and 23 cases
83 have been reported to date¹⁸. Genetic mismatches, particularly in the major histocompatibility
84 complex (MHC) genes should lead to rejection of these transmissible tumors. Consequently, the
85 role of devil MHC has been a focus of numerous studies (**Figure 1, Table S1**) to understand the

86 lack of rejection of the transmissible tumors. These studies have revealed that the DFT1 cells
87 downregulate MHC class I (MHC-I) expression ¹⁹, a phenomenon observed in many human
88 cancers ²⁰. In contrast to DFT1 cells, the DFT2 cells do express MHC-I ²¹. DFT1 and DFT2
89 cells also have 2,884 and 3,591 single nucleotide variants, respectively, that are not present in 46
90 normal devil genomes ²². The continual transmission of DFT1 and DFT2, despite MHC-I
91 expression by DFT2 cells and genetic mismatches between host and tumor, suggests that
92 additional pathways are likely involved in immune evasion.

93 Human cancer treatment has been revolutionized in the past decade by manipulating
94 interactions among immune checkpoint molecules ^{23,24}. These have proven broadly effective in
95 part because they function across many different MHC types and tumor mutational patterns.
96 However, these pathways have received little attention in transmissible cancers and other
97 naturally occurring cancers in non-model species (**Figure 1, Table S1**) ²⁵⁻²⁷. We have previously
98 shown that the inhibitory immune checkpoint molecule programmed death ligand 1 (PDL1) is
99 expressed in the DFT microenvironment and is upregulated by interferon-gamma (IFN γ) *in vitro*
100 ²⁵. This finding led us to question which other immune checkpoint molecules play a role in
101 immune evasion by the transmissible cancers and the devil's high spontaneous cancer incidence.
102 Understanding this immune evasion in a natural environment has the potential to help protect this
103 endangered species and identify protein interactions that are conserved across divergent species
104 to improve translational success of animal models ²⁷. Unfortunately, a persistent limitation for
105 immunology in non-traditional study species is a lack of species-specific reagents. Wildlife
106 biologists and veterinarians are at the front lines of emerging infectious disease outbreaks, but
107 they often lack species-specific reagents to fulfil the World Health Organization's call for "cross-
108 cutting R&D preparedness" and perform mechanistic immunological investigations ²⁸.

109 To solve the paucity of reagents available for Tasmanian devils and address ongoing
110 limitations for non-traditional study species, we developed a Fluorescent Adaptable Simple
111 Theranostic (FAST) protein system that builds upon the diverse uses of fluorescent proteins
112 previously reported^{29–33}. This simple system can be used for rapid development of diagnostic
113 and therapeutic (i.e. theranostic) immunological toolkits for any animal species (**Figure 2**). We
114 demonstrate the versatility and impact of the FAST system by using it to confirm seven receptor-
115 ligand interactions among twelve checkpoint proteins in devils.

116 In humans, these checkpoint proteins have been targets of immunotherapy in clinical
117 trials, but the functional role and binding patterns of these proteins are unknown for most other
118 species. We have used the FAST system to show that the inhibitory checkpoint protein CD200 is
119 highly expressed on DFT cells, opening the door to single-cell phenotyping of circulating tumor
120 cells (CTCs) in devil blood. Furthermore, we are the first to report that co-expression of
121 CD200R1 can block surface expression of CD200 in any species. Understanding how clonal
122 tumor cells graft onto new hosts, evade immune defenses and metastasize within a host will
123 identify evolutionarily conserved immunological mechanisms to help improve cancer, infectious
124 disease, and transplant outcomes for human and veterinary medicine.

125

126 **RESULTS**

127 **Fluorescent fusion proteins can be secreted from mammalian cells**

128 Initially, we developed FAST proteins to determine whether monomeric fluorescent
129 proteins could be fused to devil proteins and secreted from mammalian cells (**Figure 2A** and
130 **Table S2**). We used 41BB (TNFRSF9) for proof-of-concept studies by fusing the extracellular
131 domain of devil 41BB checkpoint molecule to monomeric fluorescent proteins (**Figure 2A-B**

132 and **Figure S1**). We used wild-type Chinese hamster ovary (CHO) cells and CHO cells
133 transfected with 41BBL (TNFSF9) to confirm specificity of the 41BB FAST proteins and
134 demonstrate that the fluorescent proteins (mAzurite, mCerulean3, mCherry, mCitrine, mOrange,
135 Neptune2, and mTag-BFP (aka mBFP)) remained fluorescent when secreted from mammalian
136 cells (**Figure 2C**).

137 We chose mCherry, mCitrine, mOrange, and mBFP for ongoing FAST protein
138 development. Initial batches of FAST proteins were purified using the 6xHis-tag and eluted with
139 imidazole. The gradient of FAST protein in the collection tubes was apparent when excited with
140 blue light and visualized with an amber filter unit (**Figure 2D**), allowing immediate confirmation
141 that the fluorescent protein DNA coding sequences were in-frame and the proteins were properly
142 folded. mCherry was visible without excitation or filters (**Figure 2E**). After combining,
143 concentrating, and sterile filtering the eluted fractions, 100 μ L was aliquoted and visualized
144 again using blue light to confirm fluorescent signal (**Figure 2F**). A full step-by-step protocol and
145 set of experimental templates for creating and testing FAST proteins for any species is available
146 online with the supplementary material.

147 **Receptor-ligand binding confirmed in single-step staining assays**

148 We chose additional immune checkpoint molecules for FAST protein development
149 (**Figure 3A**) based on targets of clinical trials and sequence analysis of devil genes^{27,34,35}. We
150 transfected the FAST protein expression vectors (**Table S2**) into CHO cells and tested the
151 supernatant against CHO cell lines expressing full-length receptors. 41BB FAST proteins in
152 supernatant exhibited strong binding to 41BBL cell lines, but the fluorescent signals from most
153 other FAST proteins were too weak to confirm binding to the expected receptors (**Figure S2**). As
154 FAST proteins do not require secondary reagents, we next incubated target cells with purified

155 FAST proteins and added chloroquine to block the lysosomal protein degradation pathway³⁶.
156 This allowed us to take advantage of receptor-mediated endocytosis, which can allow
157 accumulation of captured fluorescent signals inside the target cells³⁷. This protocol adjustment
158 allowed confirmation that CD47-mCherry, CD200-mBFP, CD200-mOrange, CD200R1-mBFP,
159 and CD200R1-mOrange, and PD1-mCitrine bound to their expected receptors (**Figure 3B**). We
160 also demonstrated the flexibility of the FAST proteins by showing that alternative fusion
161 conformations (**Figure S1C-D**), such as type II proteins (e.g. mCherry-41BBL) and a devil Fc-
162 tag (e.g. CD80-Fc-mCherry) bound to their expected ligands (**Figure 3B**). The stability of the
163 fusion proteins was demonstrated using supernatants that were stored at 4 °C for two months
164 prior to use in a one-hour live-culture assay with chloroquine (**Figure S3**).

165 **Cell lines secreting FAST proteins confirm protein interactions in live coculture assays**

166 To further streamline the reagent development process, we next took advantage of the
167 single-step nature of FAST proteins (i.e. no secondary antibodies or labels needed) in live-cell
168 coculture assays (**Figure 4A**). Cell lines secreting 41BB-mCherry, 41BBL-mCherry, or CD80-
169 Fc-mCherry FAST proteins were mixed with cell lines expressing full-length 41BB, 41BBL, or
170 CTLA4-mCitrine and cocultured at a 1:1 ratio overnight with chloroquine. Singlet cells were
171 gated (**Figure 4B**) and binding of mCherry FAST proteins to CFSE or mCitrine-labelled target
172 cells was analyzed (**Figure 4C**). The strongest fluorescent signal from 41BB-mCherry, 41BBL-
173 mCherry and CD80-Fc-mCherry were detected when cocultured with their predicted receptors,
174 41BBL, 41BB and CTLA4, respectively.

175 **Optimization of the FAST-Fc construct**

176 The fluorescent binding signal of CD80-Fc-mCherry was lower than expected, so we
177 next re-examined our Fc-tag construct. In humans and all other mammals examined to date the

178 IgG heavy chain has glycine-lysine (Gly-Lys) residues at the C-terminus³⁸; the initial devil IgG
179 constant region sequence available to us had an incomplete C-terminus, and thus our initial
180 CD80-Fc-mCherry vector did not have the C-terminal Gly-Lys. We subsequently made a new
181 FAST-Fc construct with CTLA4-Fc-mCherry, which exhibited strong binding to both CD80 and
182 CD86 transfected DFT cells (**Figure 4D**).

183 **CD200 mRNA and protein are highly expressed in DFT cells**

184 Analysis of previously published devil and DFT cell transcriptomes suggested that
185 CD200 mRNA is highly expressed in DFT2 cells and peripheral nerves, moderately expressed in
186 DFT1 cells, and lower in other healthy devil tissues (**Figure 5A**)^{34,35,39}. As CD200 is an
187 inhibitory molecule expressed on most human neuroendocrine neoplasms⁴⁰, and both DFT1 and
188 DFT2 originated from Schwann cells^{35,41}, we sought to investigate CD200 expression on DFT
189 cells at the protein level. Staining of wild-type DFT1 and DFT2 cells with CD200R1-mOrange
190 FAST protein showed minimal fluorescent signal (**Figure 5B**). However, overexpression of
191 CD200 using a human EF1 α promoter yielded a detectable signal with CD200R1-mOrange
192 binding to CD200 on DFT1 cells. A weak signal from CD200-mOrange was detected on DFT1
193 cells overexpressing CD200R1 (**Figure 5B**). To confirm naturally-expressed CD200 on DFT
194 cells we digested CD200 and 41BB FAST proteins using TEV protease to remove the linker and
195 fluorescent reporter. The digested proteins were then used to immunize mice for polyclonal sera
196 production. We stained target CHO cell lines with pre-immune (PI) or immune (I) mouse sera
197 collected after 3X immunizations. Only the immune sera showed strong binding to the respective
198 CD200 and 41BB target cell lines (**Figure 5C**). After the final immunization (4X), we collected
199 another batch of sera and tested it on DFT1 and DFT2 cells (**Figure 5D**). In agreement with the

200 transcriptomic data for DFT cells³⁴, the polyclonal sera revealed high levels of CD200 on DFT
201 cells, but low levels of 41BB.

202 **Overexpression of CD200R1 blocks surface expression of CD200**

203 In humans, overexpression of some checkpoint proteins can block surface expression of
204 heterophilic binding partners in *cis* (e.g. CD80 and PDL1)^{42,43}. As a potential route for
205 disrupting the inhibitory effects of CD200 on anti-tumor immunity, we tested if overexpression
206 of CD200R1 on DFT cells could reduce CD200 surface expression. We stained a DFT1 strain
207 C5065, and DFT1 C5065 cells transfected to overexpress CD200 or CD200R1 with polyclonal
208 anti-CD200 sera and secondary anti-mouse IgG AF647. We detected no surface protein
209 expression of CD200 DFT1 cells overexpressing CD200R1 (**Figure 5E**).

210 **Identification of DFT cells in whole blood using anti-CD200**

211 In addition to high expression of CD200 on neuroendocrine neoplasms^{40,44}, CD200 is
212 used as a diagnostic marker for several human blood cancers⁴⁵⁻⁴⁷. DFT cells metastasize in the
213 majority of cases⁴⁸ and our transcriptome results (**Figure 5A**) suggest that CD200 mRNA is
214 more highly expressed in DFT cells than in peripheral blood mononuclear cells (PBMCs)^{34,35}.
215 As a result, we tested if CD200 could be used to identify DFT cells in blood. We stained PBMCs
216 and DFT2 cells separately with polyclonal anti-CD200 sera and anti-mouse AlexaFluor 647 and
217 then analyzed CD200 expression by flow cytometry (**Figure S4A**). We then mixed the stained
218 PBMCs and DFT2 cells at ratios of 1:10 (**Figure S4A**) and 1:5 (**Figure S4B**) and analyzed the
219 mixed populations. PBMCs showed minimal CD200 expression and background staining
220 (**Figure S4**), whereas CD200 was highly expressed on DFT2 cells. CD200+ DFT2 cells were
221 readily distinguishable from PBMCs.

222 As our RNAseq results only included mononuclear cells, we next performed a pilot test
223 to determine if DFT cells could be spiked into whole devil blood and identified via flow
224 cytometry using CD200 staining. DFT1 and DFT2 cells were labeled with CellTrace violet
225 (CTV) and 10,000 cells were diluted directly into 100 μ L of whole blood from a healthy devil
226 (n=1/treatment; n = 1 devil). The cells were then stained with purified polyclonal anti-CD200
227 with and without secondary anti-mouse IgG AF647 prior to red blood cell (RBC) lysis. Initial
228 results showed that DFT2 cells expressed CD200 above the leukocyte background, but that
229 DFT1 cells could not be distinguished from leukocytes (**Figure S5**). To eliminate the secondary
230 antibody step from the whole blood staining protocol we next labelled the polyclonal anti-CD200
231 and normal mouse serum (NMS) with a no-wash Zenon mouse IgG AF647 labeling reagent (n =
232 1/treatment; n = 2 devils). This system again showed that CD200 expression could be used to
233 identify DFT2 cells in blood (**Figure 6**), suggesting that CD200 is a candidate marker for
234 identification of metastasizing DFT2 cells.

235

236 **DISCUSSION**

237 Naturally occurring cancers provide a unique opportunity to study immune evasion and
238 the metastatic process across diverse hosts and environments. The exceptionally high cancer rate
239 in Tasmanian devils coupled with the two transmissible tumors currently circulating in the wild
240 warrants a thorough investigation of the devil immune system. However, taking advantage of
241 such natural disease models has been out of reach for most species due to a lack of reagents. The
242 FAST protein system we developed here is well-suited to discovering additional DFT markers,
243 and more generally, filling the reagent gap for non-traditional species. For proteins like 41BB
244 that have high affinity for 41BBL, FAST proteins can be used as detection reagents directly from

245 supernatant. For other molecules with lower receptor-ligand affinity, the FAST proteins can be
246 purified, digested with a protease to remove the non-target proteins and used for production of
247 polyclonal or monoclonal antibodies.

248 The simple cut-and-paste methods for vector assembly lend the FAST protein system to
249 entry level immunology and molecular biology skill sets. Additionally, the ability of FAST
250 proteins to be used in live coculture assays and with elimination of secondary reagents, will
251 increase efficiency and reduce experimental error for advanced human and mouse cancer
252 immunology studies. For example, previous high-throughput studies have used a two-step
253 staining process (i.e. recombinant protein + secondary antibody) to screen more than 2000
254 protein interactions^{49,50}; this type of assay can be streamlined using FAST proteins to eliminate
255 the need for secondary antibodies. Fc-tags or other homodimerization domains can be
256 incorporated into FAST proteins to increase binding for low-affinity interactions.

257 Production of recombinant proteins in cell lines that closely resemble the physiological
258 conditions of the native cell type (i.e. mammalian proteins produced in mammalian cell lines) are
259 more likely to yield correct protein folding, glycosylation, and function than proteins produced
260 using evolutionarily distant cell lines⁵¹. The fluorescent fusion proteins developed here that take
261 advantage of natural receptor expression and cycling processes (e.g. CTLA4 transendocytosis) in
262 eukaryotic target cells; bacterial protein production methods are not amenable to coculture with
263 eukaryotic target cells in immunological assays⁵². Our demonstration of the FAST protein
264 system in CHO cells, which are used to produce approximately 70% of recombinant
265 pharmaceutical proteins⁵³, suggest that this method can be efficiently integrated into existing
266 research and development pipelines for humans and other vertebrate species.

267 A primary question in transmissible tumor research is why genetically mismatched cells
268 are not rejected by the host. Successful infection of devils with DFT cells relies on the ability of
269 the tumor allograft to evade and manipulate host defences. The "missing-self" hypothesis
270 suggests that the lack of constitutive MHC-I expression on DFT1 cells should lead to natural
271 killer (NK) cell-mediated killing of the allograft tumor cells. Here we used the FAST protein
272 system to develop a tool set to address this question and show that DFT1 and DFT2 cells express
273 CD200 at higher levels than most other devil tissues examined to date. CD200 has been shown to
274 directly inhibit NK cells in other species ⁵⁴⁻⁵⁶, so overexpression of CD200 is a potential
275 mechanism of immune evasion of NK responses by DFT cells.

276 We hypothesize that CD200 could be particularly important in DFT transmission as the
277 CD200-CD200R pathway is critical to the initial stages of establishing transplant and allograft
278 tolerance in other species ⁵⁷⁻⁵⁹. In line with this hypothesis, a recent study reported that
279 overexpressing several checkpoint molecules, including CD200, PDL1, and CD47, in mouse
280 embryonic stem cells could be used to generate teratomas that could establish long-term
281 allograft tolerance in fully immunocompetent hosts ⁶⁰. We have previously reported that PDL1
282 mRNA and protein are upregulated on DFT2 cells in response to IFN γ ²⁵, and our transcriptome
283 results show that CD47 is expressed at moderate to high levels in DFT cells. Here we show that
284 overexpression of CD200R1 on DFT1 eliminates binding of our polyclonal anti-CD200
285 antibodies, suggesting that DFT cells overexpressing CD200R1 could be used to test the role of
286 CD200 in allograft tolerance. Alternatively, genetic ablation of CD200 in DFT cells could be
287 used as a complementary approach to examine the role of immune checkpoint molecules in DFT
288 allograft tolerance. The CD200-CD200R1 pathway has been implicated in reducing IFN γ
289 production by dendritic cells ⁵⁹ and decreasing the responsiveness of myeloid cells to IFN γ

290 stimulation⁶¹. Low MHC-I expression is a primary means of immune evasion by DFT1 cells,
291 and disrupting the CD200-CD200R1 pathway could facilitate improved recognition of DFT1
292 cells by CD8 T cells by enhancing IFN γ -mediated MHC-I upregulation. Recent work in mice has
293 identified immunosuppressive natural regulatory plasma cells that express CD200, LAG3, PDL1,
294 and PDL2; we have previously identified PDL1+ cells with plasma cell morphology near or
295 within the DFT microenvironment²⁵.

296 Previous DFT vaccine efforts have used killed DFT cells with adjuvants^{62,63}. A similar
297 approach to treat gliomas in dogs reported that tumor-lysate with CD200 peptides nearly doubled
298 progression-free survival compared to tumor lysate alone⁶⁴. Like devils, several breeds of dog
299 are prone to cancer and these genetically-outbred large animal models provide a fertile ground
300 for testing cancer therapies. Interestingly, the CD200 peptides are reported to provide agonistic
301 function through CD200-like activation receptors (CD200R4) rather than by blocking CD200R1
302^{44,64}. The functional role of CD200-CD200R pathway in devils remains to be elucidated, but the
303 CD200R1_{NPLY} inhibitory motif and key tyrosine residues are conserved in devil CD200R^{27,65,66},
304 demonstrating this motif is conserved over 160 million years of evolutionary history⁶⁷. In
305 addition to agonistic peptides, several other options for countering CD200-CD200R immune
306 inhibition are possible. Human chronic lymphocytic leukemia cells often express high levels of
307 CD200, which can be downregulated in response to imiquimod⁶⁸. Likewise, we have previously
308 shown that DFT1 cells downregulate expression of CD200 mRNA *in vitro* in response to
309 imiquimod treatment³⁴.

310 In mice, chronic salmonella and schistosoma infections upregulated both CD200 and
311 CD200R⁶⁹. Several viruses, including cytomegalovirus⁷⁰ and herpesvirus⁷¹ manipulated the
312 CD200-CD200R pathway as a means of immune evasion. Interestingly, in one of the longest

313 running and most in-depth studies of host-pathogen coevolution, CD200R was shown to be
314 under selection in rabbits in response to myxoma virus biocontrol agent⁷². As DFT1 and DFT2
315 have been circulating in devils for more than 20 years and 5 years, respectively, it will be
316 important to monitor CD200/R expression and the potential evolution of paired activating and
317 inhibitory receptors in these natural disease models⁷³.

318 Immunophenotyping and single-cell RNAseq of circulating tumor cells (CTCs) has
319 potential to identify key gene expression patterns associated with metastasis and tissue invasion.
320 Periaxin (PRX) is the most sensitive and specific marker for DFT1 cells in
321 immunohistochemistry assays⁷⁴. Unfortunately, PRX is expressed primarily in the cytoplasm,
322 which eliminates the possibility of using PRX as a marker to sort live cells via flow cytometry
323 for single-cell RNAseq. However, CD200 is a potential marker for the identification of
324 circulating tumor cells (CTCs) from devil blood. As proof of concept, DFT2 cells could be
325 identified in devil blood spiked with DFT2 cells. As CTCs are likely to be rare in the blood of
326 most infected devils, CD200 alone would be insufficient for identifying DFT1 cells. Additional
327 surface DFT markers would be required to purify CTCs for metastases and tissue invasion
328 analyses. The FAST protein system provides a simple procedure to facilitate the production of a
329 panel of DFT-markers to help identify key proteins in the metastatic process.

330 In summary, the simple “cut-and-paste” production of the vectors and single-step testing
331 pipeline of the FAST system provided multiple benefits. The FAST system allowed us to
332 characterize receptor-ligand interactions, and to identify evolutionarily conserved immune
333 evasion pathways in naturally occurring transmissible cancers. Our initial implementation of the
334 system confirmed numerous predicted protein interactions for the first time in a marsupial
335 species and documented high expression of the inhibitory molecule CD200 on DFT cells. The

336 high expression of CD200 in devil nervous tissues and neuroendocrine tumors, downregulation
337 of CD200 in response to imiquimod, and binding of CD200 to CD200R1, is consistent with
338 results from human and mouse studies. Consequently, the CD200/R pathway provides a
339 promising immunotherapy and vaccine target for DFTs. Beyond this study, FAST proteins meet
340 the key attributes needed for reagent development, such as being straightforward to make, stable,
341 versatile, renewable, cheap, and amenable to high-throughput testing⁷⁵. The direct fusion of the
342 reporter protein to the protein-of-interest allows for immediate feedback during transfection,
343 supernatant testing, and protein purification; proteins with frameshifts, introduced stop codons,
344 or folded improperly will not fluoresce and can be discarded after a simple visualization, rather
345 than only after extensive downstream testing. Efficient mapping of immune checkpoint
346 interactions across species can identify evolutionarily conserved immune evasion pathways and
347 appropriate large animal models with naturally occurring cancer. This knowledge could inform
348 veterinary and human medicine in the fields of immunological tolerance to tissue transplants,
349 infectious disease, and cancer.

350

351 **MATERIALS AND METHODS**

352 **Study design**

353 The objectives of this study were to fill a major gap in our understanding of the
354 mammalian immune system and to understand how genetically mismatched transmissible tumors
355 evade host immunity. To achieve this goal, we developed a recombinant protein system that
356 directly fuses proteins-of-interest to a fluorescent reporter protein. The first phase was to
357 determine if the fluorescent protein remained fluorescent after secretion from mammalian cells
358 and to confirm that proteins bound to their predicted receptors (i.e. ligands). Initial testing was

359 performed in CHO cells and follow-up assays used devil cells. To further demonstrate the
360 functionality of this system for antibody development, mice were immunized with either 41BB
361 or CD200 proteins. Pre- and post-immunization polyclonal sera was used to confirm that the
362 proteins used for immunization induced antibodies that specifically bound to surface-expressed
363 recombinant proteins and native proteins on devil facial tumor cells.

364 **Target transcript amplification**

365 Target gene DNA sequences for vector construction were retrieved from Genbank,
366 Ensembl or de novo transcriptome assemblies (**Table S2**)⁷⁶. Target DNA was amplified from a
367 cDNA template or existing plasmids using primers and PCR conditions shown in **Tables S2-S4**
368 using Q5 High-Fidelity 2X Master Mix (New England Biolabs # M0494L). Primers were
369 ordered with 5' base extensions that overlapped expression vectors on either side of the
370 restriction sites. The amplified products were identified by gel electrophoresis and purified using
371 Nucleospin PCR and Gel Clean Up Kit (Macherey-Nagel # 740609.5). Alternatively, DNA
372 sequences were purchased as double stranded DNA gblocks (**Table S5**) (Integrated DNA
373 Technologies) for direct assembly into expression vectors.

374 **Construction of all-in-one Sleeping Beauty transposon vectors**

375 All new plasmids were assembled using NEBuilder kit (NEB # E5520S) following the
376 manufacturer's recommendations unless otherwise noted. DNA inserts, digested plasmids, and
377 NEBuilder master mix were incubated for 60 minutes at 50 °C and then transformed into DH5 α
378 included with the NEBuilder kit. Plasmid digestions were performed following manufacturer
379 recommendations and generally subjected to Antarctic phosphatase (New England Biolabs #
380 M0289S) treatment to prevent potential re-annealing. Sleeping Beauty transposon vectors pSBbi-
381 Hyg (Addgene # 60524), pSBbi-BH (Addgene # 60515), pSBtet-Hyg (Addgene # 60508),

382 pSBtet-RH (Addgene # 60500) were gifts to Addgene from Eric Kowarz ⁷⁷. The
383 pCMV(CAT)T7-SB100 containing the CMV promoter and SB100X transposase was a gift to
384 Addgene from Zsuzsanna Izsvak (Addgene # 34879) ⁷⁸. We first constructed an all-in-one
385 Sleeping Beauty vector by inserting a CMV promoter and SB100X transposase from
386 pCMV(CAT)T7-SB100 ⁷⁸ into pSBi-BH ⁷⁷ (**Tables S3-S4**). This was accomplished by using
387 pAF111-vec.FOR and pAF111.1.REV primers to amplify an overlap region from pSBbi-BH
388 (insert 1) and pAF111-2.FOR and pAF111-2.REV to amplify the CMV-SB100X region from
389 pCMV(CAT)T7-SB100 (insert 2). The purified amplicons were then used for NEBuilder
390 assembly of pAF111. The final all-in-one vectors pAF112 (hygromycin resistance and
391 luciferase) and pAF123 (hygromycin resistance) were assembled from the pAF111 components.
392 pAF112 was assembled by amplifying the Luc2 luciferase gene (insert 1) from pSBtet-Hyg and
393 the P2A-hygromycin resistance gene (insert 2) from pSBbi-BH and inserting into the pAF111
394 Bsu36I digest using NEBuilder. pSBbi-Hyg was Bsu36I-digested to obtain the hygromycin
395 resistance gene, and this fragment was inserted into Bsu36I-digested pAF111 using T4 ligase
396 cloning to replace the BFP-P2A-hygromycin segment in pAF111.

397 **Construction of full-length protein vectors**

398 All full-length gene coding sequences except CTLA4 were cloned into the a pAF112 SfiI
399 digest (**Table S2**). All full-length vectors also contain luciferase with T2A peptide linked to the
400 hygromycin resistance protein; luciferase was included for use in downstream functional testing
401 that was not part of this study. Tasmanian devil CTLA4 was cloned into a NotI-HF and XmaI
402 digest of pAF100 that was used in a different study but is derived from vectors pAF112 and
403 pAF138. Additionally, we also used devil PDL1 (CHO.pAF48) and 41BBL (CHO.pAF56) cell
404 lines developed using a vector system described previously ²⁵.

405 **Construction of FAST protein vectors**

406 Plasmids containing fluorescent protein coding sequences mCerulean3-N1 (Addgene #
407 54730), mAzurite-N1 (Addgene # 54617), mOrange-N1 (Addgene # 54499), mNeptune2-N1
408 (Addgene # 54837) were gifts to Addgene from Michael Davidson. mTag-BFP was amplified
409 from pSBbi-BH, mCitrine was amplified from pAF71, and mCherry was amplified from pTRE-
410 Dual2 (Clontech # PT5038-5). pAF137 was constructed by amplifying the devil 41BB
411 extracellular domain with primers pAF137-1.FOR and pAF137-1.REV and amplifying mCherry
412 with pAF137-2a.FOR and pAF137-2.REV (**Table S3-4**). 5' extensions on pAF137-1.FOR and
413 pAF137-2.REV were used to create overlaps for NEBuilder assembly of pAF137 from a pAF123
414 SfiI-digested base vector. 3' extensions on pAF137-1.REV and pAF137-2a.FOR were used to
415 create the linker that included an XmaI/SmaI restriction site, TEV cleavage tag,
416 GSAGSAAGSGEF linker peptide, and 6x-His tag between the gene-of-interest and fluorescent
417 reporter. The GSAGSAAGSGEF was chosen due to the low number of large hydrophobic
418 residues and less repeated nucleic acids than are needed with other flexible linkers such as
419 (GGGS)₄⁷⁹. The pAF137 primer extensions also created 5' NotI and 3' NheI sites in the FAST
420 vector to facilitate downstream swapping of functional genes and to create a Kozak sequence⁸⁰
421 (GCCGCCACC) upstream of the FAST protein open-reading frame. Following confirmation of
422 correct assembly via DNA sequencing, the FAST 41BB-mCherry (pAF137) was digested and
423 used as the base vector (**Figure 2B** and **Figure S1A-B**) for development of FAST vectors with
424 alternative fluorescent proteins. This was accomplished by digestion of pAF137 with SalI and
425 NheI and then inserting PCR-amplified coding sequences for other fluorescent proteins using
426 NEBuilder (**Tables S3-S4**).

427 Type I FAST (extracellular N-terminus, cytoplasmic C-terminus) protein vectors were
428 constructed by digestion of 41BB FAST vectors with NotI and either XmaI or SmaI (**Figure 2B**
429 and **Figure S1A-B**), and then inserting genes-of-interest (**Tables S2-4**). To create an Fc-tagged
430 FAST protein we fused the extracellular domain of devil CD80 to the Fc region of the devil IgG
431 (**Figure S1C**). The Fc region was amplified from a devil IgG plasmid provided by Lynn
432 Corcoran (Walter and Eliza Hall Institute of Medical Research). All secreted FAST proteins in
433 this study used their native signal peptides, except for 41BBL. 41BBL is a type II
434 transmembrane protein in which the signal peptide directly precedes the cytoplasmic and
435 transmembrane domains of the protein (cytoplasmic N-terminus, extracellular C-terminus). As
436 type I FAST vectors cannot accommodate this domain architecture, we developed an alternative
437 base vector for type II transmembrane FAST proteins (**Figure S1D**). To increase the probability
438 of efficient secretion of type II FAST proteins from CHO cells, we used the hamster IL-2 signal
439 peptide (accession # NM_001281629.1) at the N-terminus of the protein, followed by a SalI
440 restriction site, mCherry, an NheI restriction site, 6x-His tag, GSAGSAAGSGEF linker, TEV
441 cleavage site, XmaI/SmaI restriction site, the gene-of-interest, and a PmeI restriction site
442 following the stop codon.

443 **General plasmid assembly, transformation, and sequencing**

444 Following transformation of assembled plasmids, colony PCR was performed as an initial
445 test of the candidate plasmids. Single colonies were inoculated directly into a OneTaq Hot Start
446 Quick-Load 2X Master Mix (NEB # M0488) with primers pSB_EF1a_seq.FOR
447 (atcttggttcattctcaagcctcag) and pSB_bGH_seq.REV (aggcacagtgcaggctgat). PCR was performed
448 with 60 °C annealing temperature for 25-35 cycles. Colonies yielding appropriate band sizes
449 were used to inoculate Luria broth with 100 µg/mL ampicillin for bacterial outgrowth overnight

450 at 37 °C and 200 RPM. The plasmids were purified using standard plasmid kits and prepared for
451 Sanger sequencing using BigDye Terminator v3.1 Cycle Sequencing Kit (ThermoFisher #
452 4337455) with pSB_EF1a_seq.FOR and pSB_bGH_seq.REV primers. The BigDye® Terminator
453 was removed using Agencourt CleanSEQ® (Beckman Coulter # A29151) before loading
454 samples to an Applied Biosystems® 3500XL Genetic Analyzer (Applied Biosystems) for
455 sequencing by fluorescence-based capillary electrophoresis.

456 **General cell culture conditions**

457 DFT1 cell line C5065 and DFT2 cell line JV were cultured at 35 °C with 5% CO₂ in
458 cRF10 (10% complete RPMI (Gibco # 11875-093) with 2 mM L-glutamine, supplemented with
459 10% heat-inactivated fetal bovine serum (FBS), and 1% antibiotic-antimycotic (ThermoFisher #
460 15240062). RPMI without phenol red (Sigma # R7509) was used to culture FAST protein cell
461 lines when supernatants were collected for downstream flow cytometry assays. Devil peripheral
462 blood cells were cultured in cRF10 at 35 °C with 5% CO₂. CHO cells were cultured at 37 °C in
463 cRF10 during transfections and drug selection but were otherwise cultured at 35 °C in cRF5 (5%
464 complete RPMI). For production of purified recombinant proteins, stably transfected CHO cells
465 were cultured in suspension in spinner flasks in chemically defined, serum-free CHO Ex-Cell
466 (Sigma # 14361C) media supplemented with 8 mM L-glutamine, 10 mM HEPES, 50 µM 2-ME,
467 1% (v/v) antibiotic-antimycotic, and 1 mM sodium pyruvate and without hygromycin.

468 **Transfection and Generation of Recombinant Cell Lines**

469 Stable transfections of CHO and DFT cells were accomplished by adding 3 x 10⁵ cells to
470 each well in 6-well plates in cRF10 and allowing the cells to adhere overnight. The next day, 2
471 µg of plasmid DNA was added to 100 µL of PBS in microfuge tubes. Polyethylenimine (PEI)
472 (linear, MW 25,000; Polysciences # 23966-2) was diluted to 60 µg/mL in PBS and incubated for

473 at least two minutes. 100 μ L of the PEI solution was added to the 100 μ L of plasmid DNA in
474 each tube to achieve a 3:1 ratio of PEI:DNA. The solution was mixed by gentle pipetting and
475 incubated at room temperature for 15 minutes. Whilst the solution was incubating, the media on
476 the CHO cells were replaced with fresh cRF10. All 200 μ L from each DNA:PEI mix was then
477 added dropwise to the CHO cells and gently rocked side-to-side and front-to-back to evenly
478 spread the solution throughout the well. The plates were then incubated overnight at 37 °C with
479 5% CO₂. The next day the plates were inspected for fluorescence and then the media was
480 removed and replaced with cRF10 containing 1 mg/mL hygromycin (Sigma # H0654). The
481 media was replaced with fresh cRF10 1 mg/ml hygromycin every 2-3 days for the next seven
482 days until selection was complete. The cells were then maintained in 0.2 mg/mL hygromycin in
483 cRF5 at 35 °C with 5% CO₂. Supernatant was collected 2-3 weeks post-transfection and stored at
484 4 °C for two months to assess stability of secreted FAST proteins.

485 **Protein production and purification**

486 16 days post-transfection the first batch of FAST protein cell lines were adapted to a 1:1
487 mix of cRF5 and chemically defined, serum free CHO Ex-cell media for 1-2 days to facilitate
488 adaptation of the adherent CHO cells to suspension culture in serum-free media. At least 5×10^7
489 cells were then transferred to Proculture spinner flasks (Sigma # CLS45001L, CLS4500250) and
490 stirred at 75 RPM at 35 °C in 5% CO₂ on magnetic stirring platforms (Integra Bioscience #
491 183001). Cells were maintained at a density ranging from 5×10^5 to 2×10^6 cells/ml for 8-14 days.
492 Supernatant was collected every 2-3 days, centrifuged at 3200 RCF for 10 minutes, stored at 4
493 °C, and then purified using the ÄKTA start protein purification system (GE Life Sciences #
494 29022094). The supernatant was diluted 1:1 with 20 mM sodium phosphate pH 7.4 and then
495 purified using HisTrap Excel columns (GE Life Sciences # 17-3712-05) according to the

496 manufacturer's instructions. Samples were passed through the columns using a flow rate of 2
497 mL/minute at 4 °C; all wash and elution steps were done at 1 mL/minute. Elution from HisTrap
498 columns (GE Life Sciences # 17-3712-05) was accomplished using 0.5 M imidazole and
499 fractionated into 1 ml aliquots using the Frac30 fraction collector (GE Life Sciences #
500 29023051). Fluorescence of FAST proteins was checked via brief excitation (**Figure 2D**) on a
501 blue light transilluminator with an amber filter unit. In the case of mCherry chromogenic color
502 was visible (**Figure 2E**) without excitation. Fractions containing target proteins were combined
503 and diluted to 15 mL with cold PBS, dialyzed (Sigma # PURX60005) in PBS at 4 °C, 0.22 µm
504 sterile-filtered (Millipore # SLGV033RS) and concentrated using Amicon Ultra centrifugal filter
505 units (Sigma # Z706345). The protein concentration was quantified using the 280 nm absorbance
506 on a Nanodrop spectrophotometer. Extinction coefficients using for each protein were calculated
507 using the ProtParam algorithm⁸¹. The proteins were then aliquoted into microfuge tubes and
508 frozen at -80 °C until further use. The CTLA4-Fc-mCherry protein was designed, assembled,
509 and tested separately from the other FAST proteins and was tested directly in supernatant
510 without purification.

511 **Preparation of CHO cells expressing full-length proteins for flow cytometry**

512 CHO cells expressing full-length proteins were thawed in cRF10 and then maintained in
513 cRF5 with 0.2 mg/mL hygromycin. The adherent CHO cells were washed with PBS and
514 incubated with trypsin for 5 minutes at 37 °C to remove cells from the culture flask. Trypsin was
515 diluted 5X with cRF5 and centrifuged at 200 RCF for 5 minutes. Cells were resuspended in
516 cRF5, counted (viability > 95% in all cases), and resuspended and aliquoted for assays as
517 described below.

518 **Initial staining of CHO cells with 41BB FAST protein supernatants (without chloroquine)**

519 Supernatants (cRF5) were collected from CHO cells expressing devil 41BB-extracellular
520 domain fused to either mCherry (pAF137), mCitrine (pAF138), mOrange (pAF164), mBFP
521 (pAF139), mAzurite (pAF160), mCerulean3 (pAF161), or mNeptune2 (pAF163) (**Tables S2-4**).
522 The supernatant was spun for 10 minutes at 3200 RCF to remove cells and cellular debris, and
523 then stored at 4 °C until further use. CHO cells expressing devil 41BBL (CHO.pAF56) and
524 untransfected CHO cells were prepared as described above. Flow cytometry tubes were loaded
525 with 5×10^4 target CHO cells/well in cRF5, centrifuged 500 RCF for 3 minutes, and then
526 resuspended in 200 μ L of supernatant from the 41BB FAST cell lines (n=1/treatment). The tubes
527 were then incubated for 15 minutes at 4 °C, centrifuged at 500 RCF for 3 minutes, resuspended
528 in 400 μ L of cold FACS buffer, and stored on ice until the data were acquired on a Beckman-
529 Coulter Astrios flow cytometer (**Figure 2C**). All flow cytometry data was analyzed using FCS
530 Express 6 Flow Cytometry Software version 6 (Denovo Software).

531 **Staining CHO cells with FAST protein supernatants (without chloroquine)**

532 U-bottom 96-well plates were loaded with 1×10^5 target CHO cells/well in cRF5,
533 centrifuged 500 RCF for 3 minutes, and then resuspended in 175 μ L of cRF5 supernatant from
534 FAST cell lines collected 11 days after transfection (n=1/treatment). The plates were then
535 incubated for 30 minutes at room temperature, centrifuged at 500 RCF for 3 minutes,
536 resuspended in 200 μ L of cold FACS buffer, centrifuged again and fixed with FACS fix buffer
537 (PBS, 0.02% NaN₃, 0.4% formalin, 10g/L glucose). The cells were transferred to tubes, diluted
538 with FACS buffer and analyzed on a Beckman-Coulter Astrios flow cytometer (**Figure S2**).

539 **Staining CHO cells with purified FAST proteins (with chloroquine)**

540 Purified FAST proteins were diluted to 20 μ g/mL in cRF5, aliquoted into V-bottom 96-
541 well transfer plates, and then stored at 37 °C until target cells were ready for staining. Target

542 cells were resuspended in cRF5 with 100 μ M chloroquine and 100,000 cells/well were aliquoted
543 into U-bottom 96-well plates. 100 μ L of the diluted FAST proteins (n=1/treatment, 2
544 timepoints/treatment) were then transferred from the V-bottom plates into the U-bottom 96-well
545 plates containing target cells. The final volumes and concentrations were 200 μ L/well in cRF5
546 with 50 μ M chloroquine and 2 μ g/well of FAST proteins. One set of plates was incubated at 37
547 $^{\circ}$ C for 30 minutes and another set of plates was incubated at 37 $^{\circ}$ C overnight. The cells were then
548 centrifuged 500 RCF for 3 minutes, the media decanted, and incubated for 5 minutes with 100
549 μ L of trypsin to dislodge adherent cells. The cells were then washed with 200 μ L of cold FACS
550 buffer, fixed, resuspended in cold FACS buffer, and transferred to tubes for analysis on the
551 Astrios flow cytometer (**Figure 3B**).

552 **Staining CHO cells with FAST supernatants (with chloroquine)**

553 The protocol for using FAST protein supernatants was the same above as the preceding
554 experiment except for the modifications described here. Supernatants were collected 2-3 weeks
555 post-transfection, centrifuged at 3200 RCF for 10 minutes, and stored at 4 $^{\circ}$ C for 2 months. Prior
556 to staining for flow cytometry, the supernatant was 0.22 μ m filtered. Supernatant was then
557 loaded into V-bottom 96-well plates to facilitate rapid transfer to staining plates and stored at 37
558 $^{\circ}$ C until target cells were ready for staining. Target cells were prepared as described above
559 except for being diluted in cRF5 with 100 μ M chloroquine. 2×10^5 cells/well (100 μ L) were then
560 loaded into U-bottom 96-well plates. 100 μ L of FAST protein supernatant (n=1/treatment) was
561 then transferred from the V-bottom plates to achieve 50 μ M chloroquine and the cells were then
562 incubated at 37 $^{\circ}$ C for 60 minutes. The plates were then washed, fixed, and analyzed on the
563 Astrios flow cytometer (**Figure S3**). A similar procedure was used for staining stably-transfected
564 DFT cells with CTLA4-Fc-mCherry, except that the supernatant was used fresh (**Figure 4D**).

565 **Coculture assay with full-length target and FAST protein CHO cell lines (with**
566 **chloroquine)**

567 CHO cells expressing full-length CTLA4 with a C-terminal mCitrine, and CHO cells
568 expressing full-length 41BB or 41BBL were labelled with 5 μ M CFSE; CFSE and mCitrine were
569 analyzed using the same excitation laser (488 nm) and emission filters (513/26 nm). 1×10^5
570 FAST protein-secreting cells were mixed with 1×10^5 target cells in cRF5 with 50 μ M
571 chloroquine and incubated overnight at 37 °C in 96-well U-bottom plates (**Figure 4A**). The next
572 day the cells were rinsed with PBS, trypsinized, washed, fixed, and resuspended in FACS buffer
573 prior to running flow cytometry. Cells were gated on forward and side scatter (FSC x SSC) and
574 for singlets (FSC-H x FSC-A). (**Figure 4B**). Data shown in **Figure 4C** is representative of n=3
575 technical replicates/treatment. Data was collected using a Beckman Coulter MoFlo Astrios and
576 analyzed using FCS Express.

577 **Analysis of checkpoint molecule expression in DFT cells and Tasmanian devil tissues**

578 RNAseq data was generated during previous experiments, aligned against the reference
579 Tasmanian devil genome Devil_ref v7.0 (GCA_000189315.1) and summarised into normalized
580 read counts as previously described^{34,35}. RPKM-normalized read counts were produced in R
581 using edgeR⁸². Genes were ranked from highest RPKM-normalized count to lowest RPKM-
582 normalized count, and a heat map was produced for the genes of interest using the heatmap.2
583 function of gplots. Heatmap color represents gene ranking among 18,788 predicted protein-
584 coding genes in the reference genome.

585 **Staining DFTs cell with CD200/R FAST proteins**

586 50,000 DFT cells/well were aliquoted into u-bottom 96-well plates, washed with 150 μ L
587 of cRF10, and resuspended in 100 μ L of warm cRF10 containing 100 μ M chloroquine. 5 μ g of

588 FAST protein/well was then added and mixed by pipetting. The plates were then incubated at 37
589 °C for 30 minutes. The cells were then transferred to microfuge tubes without washing, stored on
590 ice, and analyzed on a Beckman Coulter MoFlo Astrios (n=2/treatment).

591 **Polyclonal antibody development**

592 CD200 and 41BB FAST proteins were digested overnight with TEV protease (Sigma #
593 T4455) at 4 °C in PBS. The cleaved linker and 6x-His tag were then removed using a His
594 SpinTrap kit (GE Healthcare # 28-9321-71). Digested proteins in PBS were diluted 1:1 in
595 Squalvax (Oz Biosciences # SQ0010) to a final concentration of 0.1 µg/µL and was mixed using
596 interlocked syringes to form an emulsion. Immunization of BALB/c mice for antibody
597 production was approved by the University of Tasmania Animal Ethics Committee (#
598 A0014680). Pre-immune sera were collected prior to subcutaneous immunization with at least 50
599 µL of the emulsion. On day 14 post-immunization the mice were boosted using a similar
600 procedure. On day 50 the mice received a booster with proteins in IFAVax (Oz Biosciences #
601 IFA0050); mice immunized with CD200 again received subcutaneous injections, whereas 41BB
602 mice received subcutaneous and intraperitoneal injections. Pre-immune and sera collected after
603 3X immunizations were then tested by flow cytometry against CHO cells expressing either 41BB
604 or CD200. CHO cells were prepared as described above and 2×10^5 cells were incubated with
605 mouse serum diluted 1:200 in PBS for 30 minutes at 4 °C. The cells were then washed 2X and
606 stained with 50 µL of anti-mouse IgG AlexaFluor 647 diluted 1:1000 in FACS buffer. The cells
607 were then washed 2X, stained with DAPI to identify live cells, and analyzed on a Cyan ADP
608 flow cytometer (**Figure 5C**). CD200 and 41BB expression on DFT cells was tested using a
609 procedure similar to the CHO cell staining, except the sera used was collected after 4X
610 immunizations and was diluted 1:500 and analyzed on the BD FACSCanto II (**Figure 5D**).

611 **Purification of antibodies from normal mouse serum (NMS) and anti-CD200 serum**

612 Approximately 200 μ L of normal mouse serum or anti-CD200 serum day 157 (after 4X
613 immunizations) were purified using a protein G SpinTrap (GE Healthcare # 28-4083-47)
614 according to the manufacturer's instructions. Serum was diluted 1:1 with 20 mM sodium
615 phosphate, pH 7.0 binding buffer, eluted with 0.1 M glycine-HCl, pH 2.7, and the pH was
616 neutralized with 0.1 M glycine-HCl, pH 2.7. The eluted antibodies were then concentrated using
617 an Amicon Ultra 0.5 centrifugal until (Merck # UFC500308) by centrifuging at 14,000 RCF for
618 30 minutes at 4 °C and then washing the antibodies with 400 μ L of PBS twice. The protein
619 concentration was then quantified on a Nanodrop spectrophotometer at 280 nm using the
620 extinction coefficients for IgG.

621 **Testing CD200 expression on DFT cells that overexpress CD200R1**

622 50,000 DFT cells/well were aliquoted into u-bottom 96-well plates and washed with 200
623 μ L of cold FACS buffer. Purified polyclonal anti-CD200 was diluted to 2.5 μ g/mL in cold FACS
624 buffer and the cells in appropriate wells were resuspend in 100 μ L/well (0.25 μ g/well) diluted
625 antibody; wells that did not receive antibody were resuspended in 100 μ L of FACS buffer. The
626 cells were incubated on ice for 20 minutes and then washed with 200 μ L of FACS buffer. Whilst
627 incubating, anti-mouse IgG-AF647 was diluted to 1 μ g/mL in cold FACS buffer and then used to
628 resuspend cells in the appropriate wells. The plates were incubated on ice for 20 minutes, then
629 washed with 100 μ L of cold FACS buffer. The cells were then resuspended in 200 μ L of FACS
630 fix and incubated on a rocking platform at room temp for 15 minutes. The cells were then
631 centrifuged 500 RCF for 3 minutes at 4 °C, resuspended in 200 μ L FACS buffer and stored at 4
632 °C until they were analyzed on a FACSCanto II (n=2/treatment).

633 **Isolation of devil peripheral blood mononuclear cells**

634 Blood collection from Tasmanian devils was approved by the University of Tasmania
635 Animal Ethics Committee (permit # A0014599) and the Tasmanian Department of Primary
636 Industries, Parks, Water and Environment (DPIPWE). Blood was collected from the jugular vein
637 and stored in EDTA tubes for transport to the lab. Blood was processed within three hours by
638 diluting 1:1 with serum-free RPMI and then layering onto Histopaque (Sigma # 10771) before
639 centrifuging at 400 RCF for 30 minutes. The interface containing the peripheral blood
640 mononuclear cells was then collected using a transfer pipette, diluted with 50 mL of serum-free
641 RPMI and centrifuged for 5 minutes at 500 RCF. Cells were washed with again with cRF10 and
642 then either used fresh or stored at -80 °C until further use.

643 **Detecting DFT2 cells in PBMC using CD200**

644 Frozen devil PBMC were thawed and cultured in cRF10 at 35 °C with 5% CO₂ for 2
645 hours, cells were then washed in FACS buffer, counted and 3x10⁵ PBMC cells used per sample.
646 DFT2.JV cells were removed from culture flasks, counted, and 2x10⁵ cells used per sample.
647 Samples were incubated with 50 µL normal goat serum (Thermo Cat # 01-6201) diluted 1:200 in
648 FACS buffer for 15 minutes at 4 °C, 50 µL of anti-CD200 serum diluted 1:100 was added (1:200
649 final) for 30 minutes at 4 °C. Cells were then washed 2X and stained with 50 µL of anti-mouse
650 IgG AlexaFluor 647 diluted to 1 µg/mL in FACS buffer for 30 minutes at 4 °C. The cells were
651 then washed 2X, stained with DAPI (Sigma Cat # D9542) to identify live cells, and analyzed on
652 the BD FACSCanto II. PBMC and DFT cells were run separately then PBMC and DFT2 mixed
653 at a ratio of 10:1 by volume for the combined samples (n=1/treatment) (**Figure S4A**). The
654 experiment was repeated (n=1/treatment), except that PBMCs and DFT cells were mixed at a 5:1
655 ratio (**Figure S4B**).

656 **Staining of DFT cells in devil whole blood**

657 DFT1.C5065 and DFT2.JV cells were labelled with 5 μ M CellTrace violet (CTV) and
658 cultured for three days at 37 °C. On the day of the assays peripheral blood from one devil was
659 collected and stored at ambient temp for less than three hours. 100 μ L of whole blood was
660 aliquoted into 15 mL tubes and stored at ambient temperature whilst DFT cells were prepared.
661 The media on CTV-labeled DFT cells were decanted and the cells were detached from the flask
662 by incubating in 2.5 mL of TrypLE Select for 5 minutes at 37 °C. The cells were washed with
663 cRF10, resuspended in cRF10, and counted. DFT cells were then diluted to 1×10^4 cells/mL in
664 cRF10 and 100 μ L were aliquoted into appropriate 15 mL tubes containing 100 μ L of whole
665 blood. 1 μ L of purified anti-CD200 (0.5 μ g/tube) was diluted into the appropriate tubes and
666 incubated for 15 minutes at ambient temperature. Next, 0.5 μ g/tube of anti-mouse IgG AF647
667 was added to each tube. Note: 0.5 μ L (0.5 μ g) of concentrated secondary antibody was
668 accidentally added directly to the tube for the data shown in the top row and middle column of
669 **Figure S5A**; for all other tubes the secondary antibody was diluted 1:20 in PBS and 10 μ L was
670 added to each tube. The cells were then incubated for 15 minutes at ambient temperature. The
671 cells were then diluted in 1 mL ammonium chloride red blood cell (RBC) lysis buffer (150 mM
672 NH_4Cl , 10 mM KHCO_3 , 0.1 mM EDTA disodium ($\text{Na}_2\text{-2H}_2\text{O}$)) and mixed immediately gently
673 pipetting five times. The cells were incubated at ambient temperature for 10 minutes and then
674 diluted with 5 mL of PBS and centrifuged 500 RCF for 3 minutes. Some tubes contained residual
675 RBCs, so the pellet was vigorously resuspended in 5 mL of RBC lysis buffer, incubated for 5
676 minutes, diluted with 5 mL of cold FACS buffer, and centrifuged 500 RCF for 3 minutes. The
677 cells were then resuspended in 250 μ L of FACS buffer and stored on ice until analysis on a
678 Beckman Coulter MoFlo Astrios (n=1/treatment). Data were analyzed in FCS Express version 6
679 **(Figure S5)**.

680 The experiment above was repeated with the following modifications. DFT cells were
681 labelled with 5 μ M of CFSE and incubated for two days at 37 °C. On the day of the assays fresh
682 blood was collected from two devils. Purified anti-CD200 and NMS were labeled with Zenon
683 mouse IgG AF647 (ThermoFisher # Z25008) and blocked with the Zenon blocking agent. 1×10^4
684 CFSE-labeled DFT cells were diluted directly into 100 μ L of whole blood in 15 mL tubes and 12
685 μ L (2 μ L antibody, 5 μ L labeling agent, 5 μ L blocking agent) of Zenon AF647-labeled purified
686 NMS or anti-CD200 were added directly to the cells. The cells were incubated for 30 minutes at
687 ambient temperature. The cells were then gently resuspended in 2.5 mL of RBC lysis buffer and
688 incubated for 10 minutes at ambient temperature. The cells were diluted with 10 mL of PBS and
689 centrifuged 500 RCF for 3 minutes. The cells were resuspended in 1.5 mL of RBC lysis buffer
690 and incubated for another 10 minutes to lyse residual RBCs. The tubes were then resuspended in
691 9 mL of cRF10 and centrifuged 500 RCF for 3 minutes. The cells were resuspended in 350 μ L of
692 cold FACS buffer containing 200 ng/mL of DAPI and stored on ice until analysis on a Beckman
693 Coulter MoFlo Astrios (n=1/treatment for n = 2 devils) (**Figure 6**).

694

695 **ACKNOWLEDGMENTS**

696 We wish to thank Ginny Ralph for her ongoing care of Tasmanian devils, and the Bonorong
697 Wildlife Sanctuary for providing access to Tasmanian devils, and Ruth Pye for providing care
698 for devils and collecting blood samples. We would like to thank John Hayball and Georgina
699 Kalodimos for advice and assistance, Mahalia Kingsley and Nirdesh Poudel for plasmid
700 construction, Nick Blackburn for bioinformatics assistance, Lynn Corcoran for the devil IgG
701 plasmid, James Murphy for a devil IL-15 plasmid, Emily Flies for editing the manuscript, and
702 Kay Holekamp for her comments on the manuscript. **Funding:** ARC DECRA grant #

703 DE180100484, ARC Linkage grant # LP0989727, ARC Discovery grant # DP130100715,
704 Morris Animal Foundation Grant-in-Aid # D14ZO-410, University of Tasmania Foundation Dr
705 Eric Guiler Tasmanian Devil Research Grant through funds raised by the Save the Tasmanian
706 Devil Appeal (2013, 2015, 2017, 2018), and Entrepreneurs' Programme - Research Connections
707 grant with Nexvet Australia Pty. Ltd. # RC50680.

708

709 **AUTHOR CONTRIBUTIONS**

710 ASF designed the study; ALP, ASF, CEBO, PRL, and PRM developed the technology; ASF,
711 CEBO, PRL, PRM, JMD, and TLP performed the experiments; ALP performed bioinformatic
712 analyses; ALP, ASF, JMD and PRL created the figures; ALP, ASF, PRL, JMD, TLP, and GMW
713 analyzed the data; ASF wrote the manuscript and all authors edited the manuscript.

714

715 **AVAILABILITY OF DATA AND MATERIALS**

716 All data are included with the paper. The FAST base vectors (pAF92.3 pAF112.7, pAF123.1,
717 pAF137.4c1, pAF138.7, pAF139.2, pAF160.1, pAF161.3, pAF163.1, pAF164.3) will be
718 available through Addgene (deposit # 77504).

719

720 **CONFLICT OF INTEREST**

721 The authors received funding from Nexvet Australia Pty. Ltd for related studies.

722

723 **REFERENCES**

- 724 1 Albuquerque TAF, Drummond do Val L, Doherty A, de Magalhães JP. From humans to
725 hydra: patterns of cancer across the tree of life. *Biol Rev* 2018; **93**: 1715–1734.
- 726 2 Abu-Helil B, Van Der Weyden L. Metastasis in the wild: investigating metastasis in non-
727 laboratory animals. *Clin Exp Metastasis* 2019. doi:10.1007/s10585-019-09956-3.
- 728 3 Olds JE, Burrough ER, Fales-Williams AJ, Lehmkuhl A, Madson D, Patterson AJ *et al.*
729 Retrospective Evaluation of Cases of Neoplasia in a Captive Population of Egyptian Fruit
730 Bats (*Rousettus Aegyptiacus*). *J Zoo Wildl Med* 2015; **46**: 325–332.
- 731 4 Chu PY, Zhuo YX, Wang FI, Jeng CR, Pang VF, Chang PH *et al.* Spontaneous neoplasms
732 in zoo mammals, birds, and reptiles in Taiwan - A 10-year survey. *Anim Biol* 2012; **62**:
733 95–110.
- 734 5 Deus A De, Alves F, Siqueira DB De, Rameh-de-albuquerque LC. Breast Carcinoma with
735 Pulmonary Metastasis in Armadillo (*Eupharactus sexcinctus*). *Acta Sci Vet* 2018; **46**: 1–5.
- 736 6 Kruse TN, Garner MM, Bonar CJ. A Retrospective Study of Pathologic Findings in
737 Captive Rock Hyrax (*Procavia Capensis*) in the United States. *J Zoo Wildl Med* 2015;
738 **46**: 798–805.
- 739 7 Effron M, Griner L, Benirschke K. Nature and rate of neoplasia found in captive wild
740 mammals, birds, and reptiles at necropsy. *J Natl Cancer Inst* 1977; **59**: 185–198.
- 741 8 Ratcliffe HL. Incidence and nature of tumors in captive wild mammals and birds. *Am J*
742 *Cancer* 1933; **17**: 116–135.
- 743 9 Priester WA, Mantel N. Occurrence of tumors in domestic animals. Data from 12 United
744 States and Canadian colleges of veterinary medicine. *J Natl Cancer Inst* 1971; **47**: 1333–
745 1344.

- 746 10 Howlader N, Noone A, Krapcho M, Miller D, Brest A, Yu M *et al.* SEER Cancer
747 Statistics Review, 1975-2016. Bethesda, MD, United States, 2016.
- 748 11 Griner LA. Neoplasms in Tasmanian devils (*Sarcophilus harrisii*). *J Natl Cancer Inst*
749 1979; **62**: 589–595.
- 750 12 Peck SJ, Michael SA, Knowles G, Davis A, Pemberton D. Causes of mortality and severe
751 morbidity requiring euthanasia in captive Tasmanian devils (*Sarcophilus harrisii*) in
752 Tasmania. *Aust Vet J* 2019; **97**: 89–92.
- 753 13 Pearse A-M, Swift K. Allograft theory: transmission of devil facial-tumour disease.
754 *Nature* 2006; **439**: 549.
- 755 14 Pye RJ, Pemberton D, Tovar C, Tubio JMC, Dun KA, Fox S *et al.* A second transmissible
756 cancer in Tasmanian devils. *Proc Natl Acad Sci* 2016; **113**: 374–379.
- 757 15 Murgia C, Pritchard JK, Kim SY, Fassati A, Weiss RA. Clonal Origin and Evolution of a
758 Transmissible Cancer. *Cell* 2006; **126**: 477–487.
- 759 16 Fleming JM, Creevy KE, Promislow DEL. Mortality in North American Dogs from 1984
760 to 2004: An Investigation into Age-, Size-, and Breed-Related Causes of Death. *J Vet*
761 *Intern Med* 2011; **25**: 187–198.
- 762 17 Lazenby BT, Tobler MW, Brown WE, Hawkins CE, Hocking GJ, Hume F *et al.* Density
763 trends and demographic signals uncover the long-term impact of transmissible cancer in
764 Tasmanian devils. *J Appl Ecol* 2018; **55**: 1368–1379.
- 765 18 James S, Jennings G, Kwon YM, Stammnitz M, Fraik A, Storer A *et al.* Tracing the rise
766 of malignant cell lines: distribution, epidemiology and evolutionary interactions of two
767 transmissible cancers in Tasmanian devils. *Evol Appl* 2019; : eva.12831.
- 768 19 Siddle H V., Kreiss A, Tovar C, Yuen CK, Cheng Y, Belov K *et al.* Reversible epigenetic

- 769 down-regulation of MHC molecules by devil facial tumour disease illustrates immune
770 escape by a contagious cancer. *Proc Natl Acad Sci* 2013; **110**: 5103–8.
- 771 20 Yoshihama S, Roszik J, Downs I, Meissner TB, Vijayan S, Chapuy B *et al.* NLRC5/MHC
772 class I transactivator is a target for immune evasion in cancer. *Proc Natl Acad Sci* 2016;
773 **113**: 5999–6004.
- 774 21 Caldwell A, Coleby R, Tovar C, Stammnitz MR, Mi Kwon Y, Owen RS *et al.* The newly-
775 arisen devil facial tumour disease 2 (DFT2) reveals a mechanism for the emergence of a
776 contagious cancer. *Elife* 2018; **7**. doi:10.7554/eLife.35314.
- 777 22 Stammnitz MR, Coorens THH, Gori KC, Hayes D, Fu B, Wang J *et al.* The Origins and
778 Vulnerabilities of Two Transmissible Cancers in Tasmanian Devils. *Cancer Cell* 2018;
779 **33**: 607-619.e15.
- 780 23 Topalian SL, Hodi FS, Brahmer JR, Gettinger SN, Smith DC, McDermott DF *et al.*
781 Safety, Activity, and Immune Correlates of Anti-PD-1 Antibody in Cancer. *N Engl J Med*
782 2012; **366**: 2443–2454.
- 783 24 Larkin J, Chiarion-Sileni V, Gonzalez R, Grob JJ, Cowey CL, Lao CD *et al.* Combined
784 Nivolumab and Ipilimumab or Monotherapy in Untreated Melanoma. *N Engl J Med* 2015;
785 **373**: 23–34.
- 786 25 Flies AS, Bruce Lyons A, Corcoran LM, Papenfuss AT, Murphy JM, Knowles GW *et al.*
787 PD-L1 is not constitutively expressed on tasmanian devil facial tumor cells but is strongly
788 upregulated in response to IFN- γ and can be expressed in the tumor microenvironment.
789 *Front Immunol* 2016; **7**: 581.
- 790 26 Ong CEB, Lyons AB, Woods GM, Flies AS. Inducible IFN- γ Expression for MHC-I
791 Upregulation in Devil Facial Tumor Cells. *Front Immunol* 2018; **9**: 3117.

- 792 27 Flies AS, Blackburn NB, Lyons AB, Hayball JD, Woods GM. Comparative analysis of
793 immune checkpoint molecules and their potential role in the transmissible tasmanian devil
794 facial tumor disease. *Front Immunol* 2017; **8**: 513.
- 795 28 World Health Organization (WHO). WHO R&D Blueprint for action to prevent
796 epidemics. World Health Organization, 2016<http://www.who.int/blueprint/en/> (accessed 1
797 May2018).
- 798 29 Shaner NC, Campbell RE, Steinbach PA, Giepmans BNG, Palmer AE, Tsien RY.
799 Improved monomeric red, orange and yellow fluorescent proteins derived from
800 *Discosoma* sp. red fluorescent protein. *Nat Biotechnol* 2004; **22**: 1567–72.
- 801 30 Cabantous S, Terwilliger TC, Waldo GS. Protein tagging and detection with engineered
802 self-assembling fragments of green fluorescent protein. *Nat Biotechnol* 2005; **23**: 102–
803 107.
- 804 31 Cha HJ, Dalal NN, Bentley WE. Secretion of human interleukin-2 fused with green
805 fluorescent protein in recombinant *Pichia pastoris*. *Appl Biochem Biotechnol* 2005; **126**:
806 1–11.
- 807 32 Duellman T, Burnett J, Yang J. Quantitation of secreted proteins using mCherry fusion
808 constructs and a fluorescent microplate reader. *Anal Biochem* 2015; **473**: 34–40.
- 809 33 Kammertoens T, Friese C, Arina A, Idel C, Briesemeister D, Rothe M *et al.* Tumour
810 ischaemia by interferon- γ resembles physiological blood vessel regression. *Nature* 2017;
811 **545**: 98–102.
- 812 34 Patchett AL, Wilson R, Charlesworth JC, Corcoran LM, Papenfuss AT, Lyons AB *et al.*
813 Transcriptome and proteome profiling reveals stress-induced expression signatures of
814 imiquimod-treated Tasmanian devil facial tumor disease (DFTD) cells. *Oncotarget* 2018;

- 815 **9**: 15895–15914.
- 816 35 Patchett AL, Coorens THH, Darby J, Wilson R, McKay MJ, Kamath KS *et al.* Two of a
817 kind: transmissible Schwann cell cancers in the endangered Tasmanian devil (*Sarcophilus*
818 *harrisii*). *Cell Mol Life Sci* 2019; : 1–12.
- 819 36 Seglen PO, Grinde B, Solheim AE. Inhibition of the Lysosomal Pathway of Protein
820 Degradation in Isolated Rat Hepatocytes by Ammonia, Methylamine, Chloroquine and
821 Leupeptin. *Eur J Biochem* 1979; **95**: 215–225.
- 822 37 Qureshi OS, Zheng Y, Nakamura K, Attridge K, Manzotti C, Schmidt EM *et al.* Trans-
823 endocytosis of CD80 and CD86: a molecular basis for the cell extrinsic function of
824 CTLA-4. *Science* 2011; **332**: 600–603.
- 825 38 van den Bremer ET, Beurskens FJ, Voorhorst M, Engelberts PJ, de Jong RN, van der
826 Boom BG *et al.* Human IgG is produced in a pro-form that requires clipping of C-terminal
827 lysines for maximal complement activation. *MAbs* 2015; **7**: 672–680.
- 828 39 Patchett AL, Latham R, Brettingham-Moore KH, Tovar C, Lyons AB, Woods GM. Toll-
829 like receptor signaling is functional in immune cells of the endangered Tasmanian devil.
830 *Dev Comp Immunol* 2015; **53**: 123–133.
- 831 40 Love JE, Thompson K, Kilgore MR, Westerhoff M, Murphy CE, Papanicolau-Sengos A
832 *et al.* CD200 Expression in Neuroendocrine Neoplasms. *Am J Clin Pathol* 2017; **148**:
833 236–242.
- 834 41 Murchison EP, Tovar C, Hsu A, Bender HS, Kheradpour P, Rebbeck CA *et al.* The
835 Tasmanian devil transcriptome reveals schwann cell origins of a clonally transmissible
836 cancer. *Science* 2010; **327**: 84–87.
- 837 42 Haile ST, Bosch JJ, Agu NI, Zeender AM, Somasundaram P, Srivastava MK *et al.* Tumor

- 838 cell programmed death ligand 1-mediated T cell suppression is overcome by coexpression
839 of CD80. *J Immunol* 2011; **186**: 6822–9.
- 840 43 Sugiura D, Maruhashi T, Okazaki I, Shimizu K, Maeda TK, Takemoto T *et al.* Restriction
841 of PD-1 function by *cis* -PD-L1/CD80 interactions is required for optimal T cell
842 responses. *Science* 2019; : eaav7062.
- 843 44 Moertel CL, Xia J, LaRue R, Waldron NN, Andersen BM, Prins RM *et al.* CD200 in CNS
844 tumor-induced immunosuppression: The role for CD200 pathway blockade in targeted
845 immunotherapy. *J Immunother Cancer* 2014; **2**: 46.
- 846 45 Challagundla P, Medeiros LJ, Kanagal-Shamanna R, Miranda RN, Jorgensen JL.
847 Differential Expression of CD200 in B-Cell Neoplasms by Flow Cytometry Can Assist in
848 Diagnosis, Subclassification, and Bone Marrow Staging. *AJCP / Orig Artic Am J Clin*
849 *Pathol* 2014; **142**: 837–844.
- 850 46 Spacek M, Karban J, Radek M, Babunkova E, Kvasnicka J, Jaksa R *et al.* CD200
851 Expression Improves Differential Diagnosis Between Chronic Lymphocytic Leukemia
852 and Mantle Cell Lymphoma. *Blood* 2014; **124**.
- 853 47 Saksena A, Yin CC, Xu J, Li J, Zhou J, Wang SA *et al.* CD23 expression in mantle cell
854 lymphoma is associated with CD200 expression, leukemic non-nodal form, and a better
855 prognosis. *Hum Pathol* 2019; **89**: 71–80.
- 856 48 Loh R, Hayes D, Mahjoor A, O’Hara A, Pyecroft S, Raidal S. The immunohistochemical
857 characterization of devil facial tumor disease (DFTD) in the Tasmanian Devil
858 (*Sarcophilus harrisii*). *Vet Pathol* 2006; **43**: 896–903.
- 859 49 Yao S, Zhu Y, Zhu G, Augustine M, Zheng L, Goode DJ *et al.* B7-h2 is a costimulatory
860 ligand for CD28 in human. *Immunity* 2011; **34**: 729–740.

- 861 50 Wang J, Sanmamed MF, Datar I, Su TT, Ji L, Sun J *et al.* Fibrinogen-like Protein 1 Is a
862 Major Immune Inhibitory Ligand of LAG-3. *Cell* 2018; **0**.
863 doi:10.1016/J.CELL.2018.11.010.
- 864 51 Aricescu AR, Lu W, Jones EY. A time- and cost-efficient system for high-level protein
865 production in mammalian cells. *Acta Crystallogr Sect D Biol Crystallogr* 2006; **62**: 1243–
866 1250.
- 867 52 Consortium SG, Biologiques A et F des M, Center BSG, Consortium CSG, Innovation IC
868 for S and F, Center ISP *et al.* Protein production and purification. *Nat Methods* 2008; **5**:
869 135.
- 870 53 Jayapal KP, Wlaschin KF, Hu WS, Yap MGS. Recombinant protein therapeutics from
871 CHO cells - 20 years and counting. *Chem Eng Prog* 2007; **103**: 40–47.
- 872 54 Atfy M. CD200 Suppresses the Natural Killer Cells and Decreased its Activity in Acute
873 Myeloid Leukemia Patients. *J Leuk* 2015; **3**.[https://www.omicsonline.org/open-](https://www.omicsonline.org/open-access/cd200-suppresses-the-natural-killer-cells-and-decreased-its-activity-in-acutemyeloid-leukemia-patients-2329-6917-1000190.pdf)
874 [access/cd200-suppresses-the-natural-killer-cells-and-decreased-its-activity-in-](https://www.omicsonline.org/open-access/cd200-suppresses-the-natural-killer-cells-and-decreased-its-activity-in-acutemyeloid-leukemia-patients-2329-6917-1000190.pdf)
875 [acutemyeloid-leukemia-patients-2329-6917-1000190.pdf](https://www.omicsonline.org/open-access/cd200-suppresses-the-natural-killer-cells-and-decreased-its-activity-in-acutemyeloid-leukemia-patients-2329-6917-1000190.pdf) (accessed 18 Apr2019).
- 876 55 Coles SJ, Man S, Hills R, Wang EC, Burnett A, Darley RL *et al.* Over-Expression of
877 CD200 In Acute Myeloid Leukemia Mediates the Expansion of Regulatory T-
878 Lymphocytes and Directly Inhibits Natural Killer Cell Tumor Immunity. *Blood* 2015; **116**:
879 491.
- 880 56 Coles SJ, Wang ECY, Man S, Hills RK, Burnett AK, Tonks A *et al.* CD200 expression
881 suppresses natural killer cell function and directly inhibits patient anti-tumor response in
882 acute myeloid leukemia. *Leukemia* 2011; **25**: 792–9.
- 883 57 Gorczynski RM, Chen Z, Khatri I, Yu K. Graft-infiltrating cells expressing a CD200

- 884 transgene prolong allogeneic skin graft survival in association with local increases in
885 Foxp3 +Treg and mast cells. *Transpl Immunol* 2011; **25**: 187–193.
- 886 58 Gorczynski RM, Chen Z, He W, Khatri I, Sun Y, Yu K *et al.* Expression of a CD200
887 transgene is necessary for induction but not maintenance of tolerance to cardiac and skin
888 allografts. *J Immunol* 2009; **183**: 1560–1568.
- 889 59 Gorczynski L, Chen Z, Hu J, Kai Y, Lei J, Ramakrishna V *et al.* Evidence That an OX-2-
890 Positive Cell Can Inhibit the Stimulation of Type 1 Cytokine Production by Bone
891 Marrow-Derived B7-1 (and B7-2)-Positive Dendritic Cells. *J Immunol* 1999; **162**: 774–
892 781.
- 893 60 Harding J, Vintersten-Nagy K, Shutova M, Yang H, Tang JK, Massumi M *et al.* Induction
894 of long-term allogeneic cell acceptance and formation of immune privileged tissue in
895 immunocompetent hosts. Cold Spring Harbor Laboratory, 2019 doi:10.1101/716571.
- 896 61 Jenmalm MC, Cherwinski H, Bowman EP, Phillips JH, Sedgwick JD. Regulation of
897 Myeloid Cell Function through the CD200 Receptor. *J Immunol* 2014; **176**: 191–199.
- 898 62 Tovar C, Pye RJ, Kreiss A, Cheng Y, Brown GK, Darby J *et al.* Regression of devil facial
899 tumour disease following immunotherapy in immunised Tasmanian devils. *Sci Rep* 2017;
900 **7**: 43827.
- 901 63 Pye R, Patchett A, McLennan E, Thomson R, Carver S, Fox S *et al.* Immunization
902 strategies producing a humoral IgG immune response against devil facial tumor disease in
903 the majority of Tasmanian devils destined for wild release. *Front Immunol* 2018; **9**: 259.
- 904 64 Olin MR, Ampudia-Mesias E, Pennell CA, Sarver A, Chen CC, Moertel CL *et al.*
905 Treatment combining CD200 immune checkpoint inhibitor and tumor-lysate vaccination
906 after surgery for pet dogs with high-grade glioma. *Cancers (Basel)* 2019; **11**: 137.

- 907 65 Zhang S, Phillips JH. Identification of tyrosine residues crucial for CD200R-mediated
908 inhibition of mast cell activation. *J Leukoc Biol* 2005; **79**: 363–368.
- 909 66 Hatherley D, Lea SM, Johnson S, Barclay AN. Structures of CD200/CD200 receptor
910 family and implications for topology, regulation, and evolution. *Structure* 2013; **21**: 820–
911 832.
- 912 67 Luo ZX, Yuan CX, Meng QJ, Ji Q. A Jurassic eutherian mammal and divergence of
913 marsupials and placentals. *Nature* 2011; **476**: 442–445.
- 914 68 Wong KK, Khatri I, Shaha S, Spaner DE, Gorczynski RM. The role of CD200 in
915 immunity to B cell lymphoma. *J Leukoc Biol* 2010; **88**: 361–372.
- 916 69 Caserta S, Nausch N, Sawtell A, Drummond R, Barr T, MacDonald AS *et al.* Chronic
917 infection drives expression of the inhibitory receptor CD200R, and its ligand CD200, by
918 mouse and human CD4 T cells. *PLoS One* 2012; **7**: e35466.
- 919 70 Foster-Cuevas M, Westerholt T, Ahmed M, Brown MH, Barclay AN, Voigt S.
920 Cytomegalovirus e127 protein interacts with the inhibitory CD200 receptor. *J Virol* 2011;
921 **85**: 6055–9.
- 922 71 Foster-Cuevas M, Wright GJ, Puklavec MJ, Brown MH, Barclay AN. Human herpesvirus
923 8 K14 protein mimics CD200 in down-regulating macrophage activation through CD200
924 receptor. *J Virol* 2004; **78**: 7667–76.
- 925 72 Alves JM, Carneiro M, Cheng JY, Matos AL de, Rahman MM, Loog L *et al.* Parallel
926 adaptation of rabbit populations to myxoma virus. *Science* 2019; : eaau7285.
- 927 73 Barclay AN, Hatherley D. The Counterbalance Theory for Evolution and Function of
928 Paired Receptors. *Immunity* 2008; **29**: 675–678.
- 929 74 Tovar C, Obendorf D, Murchison EP, Papenfuss AT, Kreiss A, Woods GM. Tumor-

930 specific diagnostic marker for transmissible facial tumors of tasmanian devils:
931 Immunohistochemistry studies. *Vet Pathol* 2011; **48**: 1195–1203.

932 75 Marx V. Calling the next generation of affinity reagents. *Nat Methods* 2013; **10**: 829–833.

933 76 Grabherr MG, Haas BJ, Yassour M, Levin JZ, Thompson DA, Amit I *et al.* Full-length
934 transcriptome assembly from RNA-Seq data without a reference genome. *Nat Biotechnol*
935 2011; **29**: 644–52.

936 77 Kowarz E, Löscher D, Marschalek R. Optimized Sleeping Beauty transposons rapidly
937 generate stable transgenic cell lines. *Biotechnol J* 2015; **10**: 647–653.

938 78 Mátés L, Chuah MKL, Belay E, Jerchow B, Manoj N, Acosta-Sanchez A *et al.* Molecular
939 evolution of a novel hyperactive Sleeping Beauty transposase enables robust stable gene
940 transfer in vertebrates. *Nat Genet* 2009; **41**: 753–761.

941 79 Waldo GS, Standish BM, Berendzen J, Terwilliger TC. Rapid protein-folding assay using
942 green fluorescent protein. *Nat Biotechnol* 1999; **17**: 691–5.

943 80 Kozak M. An analysis of 5'-noncoding sequences from 699 vertebrate messenger RNAs.
944 *Nucleic Acids Res* 1987; **15(20)**: 8125–8148.

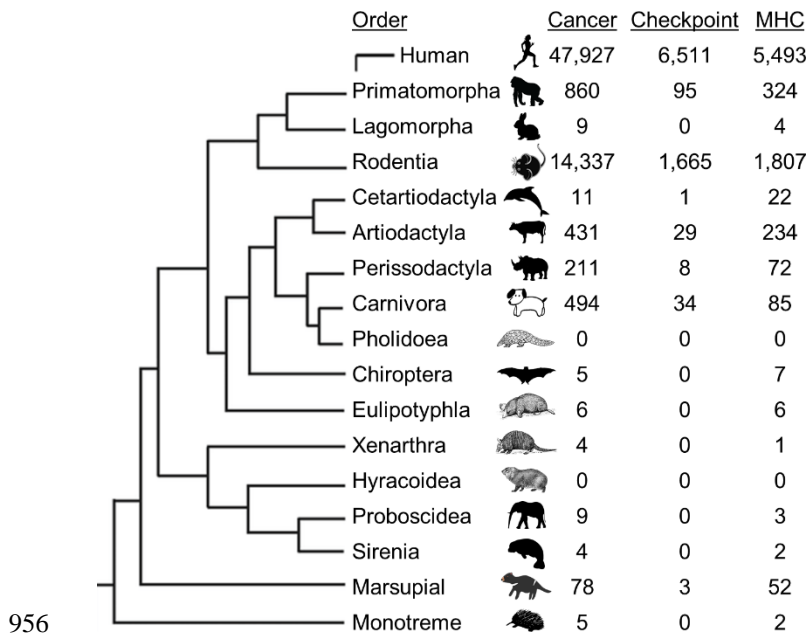
945 81 Gasteiger E, Hoogland C, Gattiker A, Duvaud S, Wilkins MR, Appel RD *et al.* Protein
946 identification and analysis tools in the ExPASy server. In: Walker JM (ed). *The*
947 *Proteomics Protocols Handbook*. Humana Press, 2005, pp 571–607.

948 82 Robinson M, McCarthy D, Smyth G. edgeR: a Bioconductor package for differential
949 expression analysis of digital gene expression data. *Bioinformatics* 2010; **26**: 139–140.

950
951
952

954 **FIGURES**

955

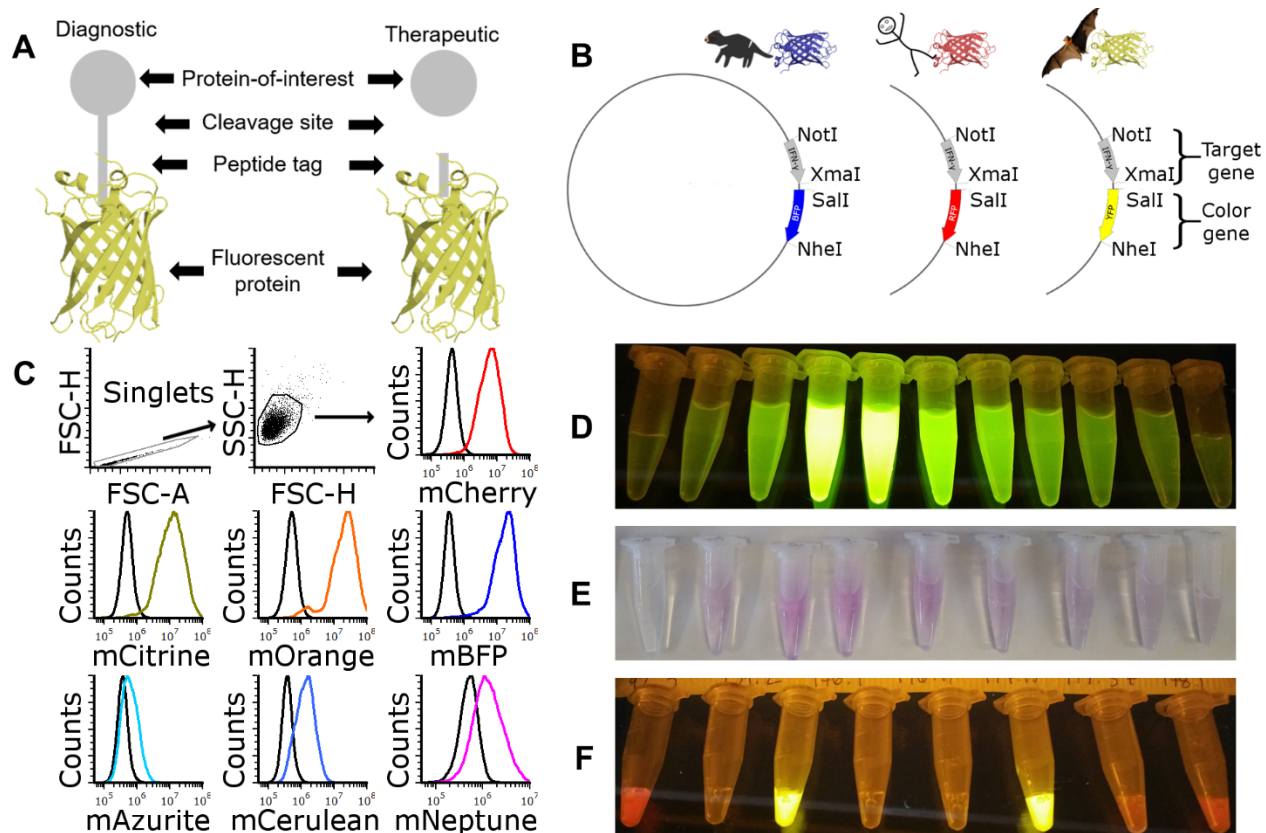


956

957

958 **Figure 1. Phylogenetic tree of immune system related studies in mammal orders 2009-2019.**

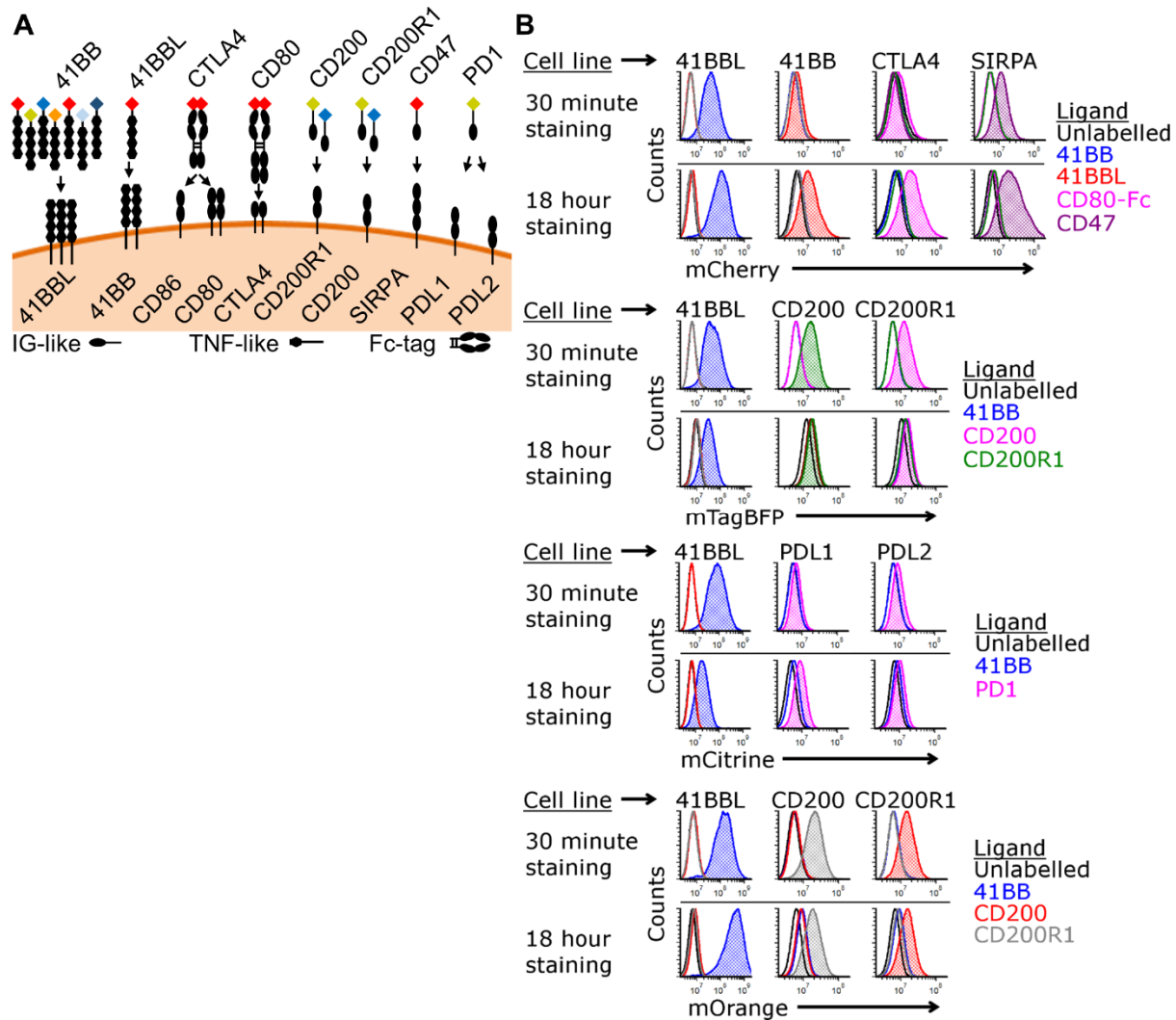
959 Metastatic cancer has been reported in nearly all mammalian orders and major histocompatibility
 960 complexes (MHC) have been the most intensely studied molecules in most orders. In the past
 961 decade, studies of immune checkpoint molecules (PD1, PDL1, CTLA4) have become a primary
 962 focus in humans and rodents. However, immune checkpoint studies in other species are limited,
 963 particularly at the protein level, due to the lack of species-specific reagents. This creates a vast
 964 gap in our understanding of the evolution of the mammalian immune system. The numbers in the
 965 columns represent the number studies matching Web of Science search results between 2009-
 966 2019. See Table S1 for search terms.



967
968 **Figure 2. FAST protein schematic and initial testing.** (A) Schematic diagram of FAST protein

969 therapeutic and diagnostic (i.e. theranostic) features and (B) vector map showing restriction sites
970 for swapping the target gene (i.e. gene-of-interest) and color genes (i.e. fluorescent protein). (C)
971 Results of flow cytometry binding assay with devil 41BB FAST proteins. The colored lines in
972 the histograms show binding of devil 41BB fused to mCherry, mCitrine, mOrange, mTagBFP,
973 mAzurite, mCerulean3, or mNeptune2 to CHO cells transfected with devil 41BBL, and the black
974 lines show binding to untransfected CHO cells. (D-E) Images showing the gradient of FAST
975 proteins eluted from HisTrap columns. (D) mCitrine excited with blue light and (E) chromogenic
976 visualization of mCherry without excitation. (F) Image of 100 μ L of FAST protein excited with
977 blue light (NOTE: mBFP appears clear with blue excitation and amber filter unit).

978



979

980 **Figure 3. Map and testing of soluble proteins FAST proteins.** (A) Diagram of soluble FAST

981 proteins and full-length proteins used for testing of FAST proteins. 41BBL is a type II

982 transmembrane protein; all other proteins are type I. CD80 and CTLA4 soluble FAST proteins

983 included a devil IgG Fc-tag. Arrows indicate interactions confirmed in this study. (B)

984 Histograms showing binding of FAST proteins to CHO cells expressing full-length devil

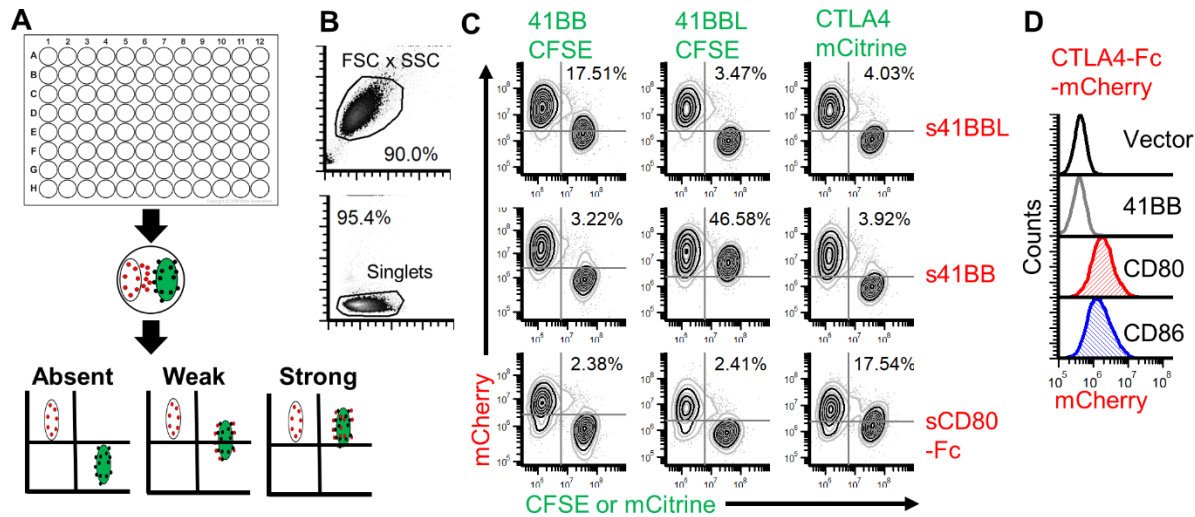
985 proteins. Target CHO cells were cultured with chloroquine to block lysosomal degradation of

986 FAST proteins and maintain fluorescent signal during live-culture binding assays with 2 μ g/well

987 of purified FAST proteins for 30 minutes or 18 hours to assess receptor-ligand binding (n=1/time

988 point).

989



990

991 **Figure 4. Live-cell coculture assays with FAST proteins.** (A) Schematic of coculture assays to

992 assess checkpoint molecule interactions (Absent, Weak, Strong). Cells were mixed and cultured

993 overnight with chloroquine. Protein binding and/or transfer were assessed using flow cytometry.

994 (B) Gating strategy for coculture assays. (C) CHO cells that secrete 41BBL-mCherry, 41BB-

995 mCherry, or CD80-Fc-mCherry were cocultured overnight with target CHO cells that express

996 full-length 41BB, 41BBL, or CTLA4. 41BB and 41BB-L were labeled with CFSE, whereas full-

997 length CTLA4 was directly fused to mCititrine. Cells that secrete mCherry FAST proteins appear

998 in the upper left quadrant. Cells expressing full-length proteins and labeled with CFSE or

999 mCititrine appear in the lower right quadrant. Cells in the upper right quadrant represent binding

1000 of mCherry FAST proteins to full-length proteins on CFSE or mCititrine labeled cells. Results

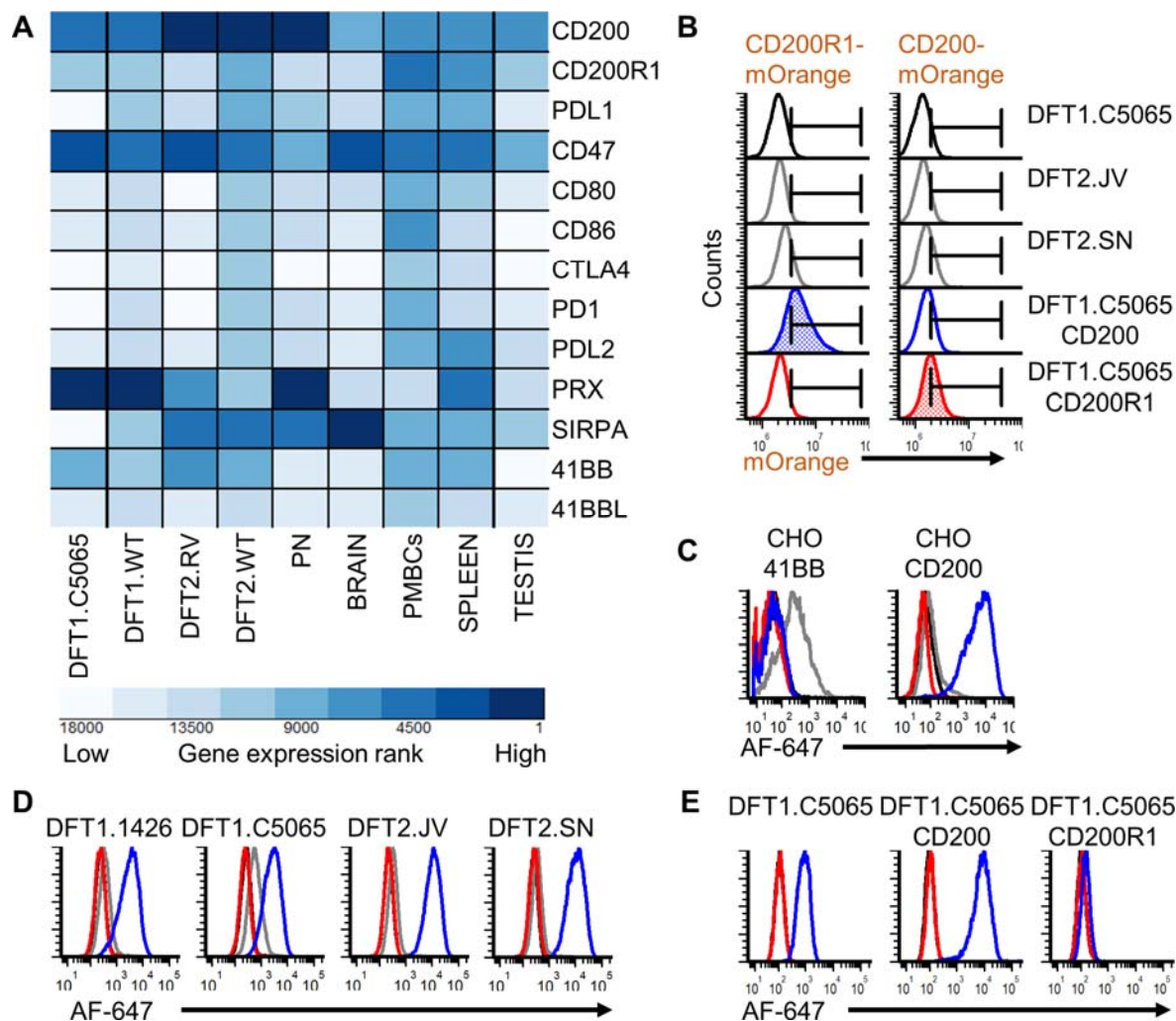
1001 shown are representative of n=3/treatment. (D) CTLA4-Fc-mCherry FAST protein binding to

1002 DFT cells. DFT1 C5065 cells transfected with control vector (black), 41BB (gray), CD80 (red),

1003 or CD86 (blue) were stained with CTLA4-Fc-mCherry supernatant with chloroquine. Results are

1004 representative of n=2 replicates/treatment.

1005

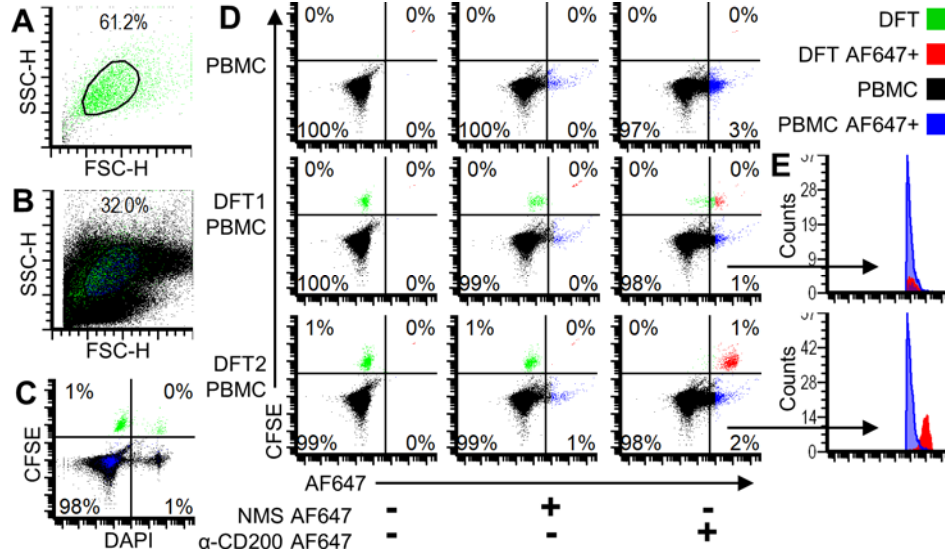


1006

1007 **Figure 5. Elevated CD200 expression on DFT cells.** (A) Heatmap showing within sample
 1008 transcript ranking (1 = highest expression) according to RPKM-normalized mRNA sequencing
 1009 counts of 18,788 annotated coding genes (devil_refv7.0; GCA_000189315.1). Genes-of-interest
 1010 for this study are plotted as heatmap with dark blue indicating the most highly expressed genes.
 1011 Technical replicates (n=2) were used for all tissues, except peripheral nerve (PN) (n=1). (B)
 1012 Wild type DFT1.C5065, DFT2.JV, DFT2.SN, and DFT1.C5065 transfected to overexpress
 1013 CD200 or CD200R1 were stained with 5 μ g of either CD200R1-mOrange or CD200-mOrange
 1014 FAST protein. Histograms filled with blue or red highlight the cells overexpressing CD200 or
 1015 CD200R1 and their expected binding interactions with CD200R1 and CD200, respectively.

1016 Target cells were cultured with FAST proteins in chloroquine, incubated 30 minutes, and run
1017 without washing. Results are representative of n=2 replicates/treatment. (C) Mice were
1018 immunized with TEV digested 41BB or CD200 FAST proteins. Black = pre-immune (PI) and
1019 gray = immune (I) sera from a mouse immunized with 41BB; red = pre-immune (PI) and blue =
1020 immune (I) sera from a mouse immunized with CD200. CHO cells transfected with either full-
1021 length 41BB or CD200 were stained with sera and then anti-mouse AlexaFluor-647. Results are
1022 representative of n=2/treatment. (D) Sera was used to screen two strains of DFT1 and two strains
1023 of DFT2 cells for 41BB and CD200 expression. PI sera was negative in all cases, whereas all
1024 DFT1 and DFT2 cells expressed CD200. Results are representative of n=3/treatment. (E) DFT1
1025 C5065 transfected with either vector control, CD200, or CD200R1 were stained with purified
1026 polyclonal anti-CD200 and anti-mouse IgG AlexaFluor 647 (black = no antibodies, red =
1027 secondary antibody only, blue = primary + secondary antibody). Results are representative of
1028 n=2/treatment.
1029

1030



1031

1032 **Figure 6. CD200 identifies DFT cells in whole blood.** Color dot plots showing DFT cells in
 1033 green (CFSE), PBMCs in black, DFT Alexa Fluor 647+ (AF647) cells in red, and PBMC
 1034 AF647+ in blue. (A) Forward- and side-scatter plot of DFT.JV cells and (B) DFT.JV cells mixed
 1035 with PBMCs. (C) Color dot plot showing dead cells stained with DAPI (right quadrants) and
 1036 CFSE-labeled DFT cells (upper quadrants). (D) The top row shows unmixed PBMCs. The
 1037 middle row and bottom row show DFT1.C5065 and DFT2.JV cells, respectively, mixed with
 1038 PBMCs. Alexa Fluor 647+ DFT (red) and PBMC (blue) are in the right quadrants. (E) Histogram
 1039 overlays to highlight AF647+ (right quadrants) from DFT1-PBMC and DFT2-PBMC mixtures.
 1040 Cells were analyzed on the Beckman-Coulter MoFlo Astrios.

1041

1042 **TABLES (See supplementary Materials)**

